농학박사 학위논문

Systematic characterization of the peroxidase gene family provides new insights into fungal pathogenicity in *Magnaporthe oryzae*

벼 도열병균 병원성에 영향을 주는

과산화효소 유전자군 특성 분석

2015년 8월

서울대학교 대학원

농생명공학부 식물미생물학전공

미르 알베리 아피파

Systematic characterization of the peroxidase gene family provides new insights into fungal pathogenicity in *Magnaporthe oryzae*

A dissertation submitted in partial
fulfillment of the requirement for
the degree of

DOCTOR OF PHILOSOPHY

to the Faculty of
Department of Agricultural Biotechnology

at

SEOUL NATIONAL UNIVERSITY

by

Mir Albely Afifa

AUGUST, 2015

농학박사 학위논문

벼 도열병균 병원성에 영향을 주는 과산화효소 유전자군 특성 분석

지도교수 이 용 환

이 논문을 농학박사 학위논문으로 제출함

2015년 6월

서울대학교 대학원
농생명공학부 식물미생물학전공
미르 알베리 아피파

미르 알베리 아피파의 박사학위 논문을 인준함
2015년 6월

위 원 장 김 성 호

부 위원장 이 용 환

위 원 [illegible] 수

위 원 강 국 형

위 원 박 숙 영

A THESIS FOR THE DEGREE OF DOCTOR OF PHILOSOPHY

Systematic characterization of the peroxidase gene family provides new insights into fungal pathogenicity in *Magnaporthe oryzae*

UNDER THE DIRECTION OF DR. YONG-HWAN LEE

SUBMITTED TO THE FACULTY OF THE GRADUATE SCHOOL OF SEOUL NATIONAL UNIVERSITY

BY

MIR ALBELY AFIFA

MAJOR IN PLANT MICROBIOLOGY
DEPARTMENT OF AGRICULTURAL BIOTECHNOLOGY

JUNE 2015

APPROVED AS A QUALIFIED THESIS OF MIR ALBELY AFIFA FOR THE DEGREE OF DOCTOR OF PHILOSOPHY BY THE COMMITTEE MEMBERS

CHAIRMAN Yong Ho Kim

VICE CHAIRMAN Yong-Hwan Lee

MEMBER Kyoung Su Kim

MEMBER Kook-Hyung Kim

MEMBER Sook-Young Park

Systematic characterization of the peroxidase gene family provides new insights into fungal pathogenicity in *Magnaporthe oryzae*

Mir Albely Afifa

ABSTRACT

Plants respond to microbial attack by the rapid generation of reactive oxygen species (ROS) as part of innate immunity. Fungal pathogens have evolved effective anti-oxidant defense system as countermeasure. Recent studies proposed peroxidases as components of antioxidant defense system. However, significance of role of fungal peroxidases during interaction with host plants has not been addressed at genomic level to date. Here, we systematically identified peroxidase genes and analyzed their impact on fungal pathogenesis in a model plant pathogenic fungus, *Magnaporthe oryzae*. Phylogeny reconstruction among 6 fungal species placed *Magnaporthe oryzae* 27 putative peroxidase genes into 15 clades. Expression profiles showed that majority of them are

responsive to *in planta* condition and *in vitro* H_2O_2 where 23 genes were up-regulated during plant infection, and 15 genes were responsive to *in vitro* H_2O_2. Among them, seven genes (*MoAPX1*, *MoAPX2*, *MoCCP1*, *MoHPX1*, *MoLDS1*, *TPX1*, and *MoPRX1*) were selected from clades that do not contain previously characterized genes for functional analysis except *TPX1*. Our analysis of individual deletion mutants for seven selected genes including *MoPRX1* revealed that these genes contribute to fungal development and/or pathogenesis. Importantly, we found significant positive correlation among sensitivity to H_2O_2, peroxidase activity and fungal pathogenicity. In-depth analysis of *MoPRX1* demonstrated that it is a functional ortholog of thioredoxin peroxidase in *Saccharomyces cerevisiae* and required for detoxification of oxidative burst within host cells. Furthermore, transcriptional profiling of other peroxidases in Δ*Moprx1* suggested interwoven nature of peroxidase-mediated anti-oxidation defense system. Taken together, this work provides overview and insights into infection strategy built on evolutionarily conserved peroxidases in the rice blast fungus.

KEY WORDS: *Magnaporthe oryzae*, peroxidase, Peroxiredoxins, evolutionary conserved gene, ROS detoxification, fungal development and pathogenicity, plant-microbe interaction.

Student number: 2011-30808

CONTENTS

Page

LIST OF TABLES

LIST OF FIGURES

Page

INTRODUCTION

In plant-pathogen interactions, one of the first defense responses in plants is rapid and transient production of reactive oxygen species (ROS) (Bolwell and Wojtaszek, 1997; Lamb and Dixon, 1997; Wojtaszek, 1997). ROS generation is spatially and temporally regulated. ROS are typically produced in the apoplastic compartment within minutes following initiation of pathogenic infection (Doke, 1983; Levine, 1994; Tenhaken *et al.*, 1994; Auh and Murphy, 1995; Grant, 2000; Brown *et al.*, 2000). ROS and intracellular redox changes can be used by pathogenic fungi for signalling purposes (Heller, 2012; Meyer *et al.*, 2012) as well as development and pathogenicity (Heller and Tudzynski, 2011; Heller *et al.*, 2012). Although O_2^- is the proximal product generated, the more stable H_2O_2 is the most abundant ROS. ROS can directly kill pathogens, produce cross-linked cell wall polymers to fortify physical barriers to pathogen entry, or act as a messenger in a cell signaling pathway, leading to pathogenesis-related (PR) gene expression and localized hypersensitive responses (Bradley *et al.*, 1992; Lamb and Dixon, 1997; Wojtaszek, 1997; Torres *et al.*, 2005; Jones and Dangl, 2006; Huckelhoven, 2007).

Pathogens must effectively incapacitate production of host-driven ROS or

detoxify ROS for successful infection in host cells (Agrios, 1992; Chai *et al.*, 2009). Studies have demonstrated that H_2O_2 detoxification is an essential virulence determinant in fungal pathogens such as *Candida albicans* (Enjalbert *et al.*, 2007), *Ustilago maydis* (Molina and Kahmann, 2007), *Alternaria alternata* (Kim, Willger *et al.*, 2009; Lin *et al.*, 2009), and *Magnaporthe oryzae* (Molina and Kahmann, 2007; Chi *et al.*, 2009a, Guo *et al.*, 2011, Samalova *et al.*, 2014). Furthermore, recent studies have identified a group of ROS-scavenging enzymes, peroxidases, as workhorses for the fungal antioxidant defense system (Missall *et al.*, 2004; Dietz *et al.*, 2006; Huang *et al.*, 2011). Peroxidases (EC1.11.1.x) are enzymes that mediate electron transfer from H_2O_2 and organic peroxide to various electron acceptors. They are evolutionarily conserved and implicated in biological processes as diverse as immune responses and hormone regulation (Fourquet *et al.*, 2008; Edgar *et al.*, 2012; Ishii *et al.*, 2012; Rhee *et al.*, 2012). Examples of peroxidase enzymes include NAD(P)H oxidase, catalase, glutathione peroxidase, catalase peroxidase, ascorbate peroxidase, lignin peroxidase, and peroxiredoxin (Passardi *et al.*, 2007).

Pathogenic fungi are becoming great threats to both plant and animal and are jeopardizing food security (Fisher *et al.*, 2012). The hemibiotrophic fungus *M. oryzae* is a causal agent of the rice blast, one of the most devastating disease in

cultivated rice (Talbot, 2003). This disease is estimated to destroy an amount of rice that would feed 60 millions of people annually (Talbot, 2003). The fungus is genetically tractable and can undergo infection-specific development in a laboratory setting. Since the full genome sequences of *M. oryzae* and rice are publicly available (Dean *et al.*, 2005), rice blast is a model system for studying plant-pathogen interactions.

The rice blast fungus experiences sequential developmental changes. The disseminated asexual spore, the conidium, attaches to the hydrophobic host surface upon hydration, and produces a cylindrical germ tube. The end of the germ tube forms a specialized dome-shaped infection structure called an appressorium. The mature heavily malanized appressorium mechanically penetrates the cuticular layer of host plants, using enormous turgor pressure (> 8 Mpa) (Howard *et al.*, 1991; Talbot, 2003). In a host plant, the fungus enters the host cytoplasm via a penetration peg, develops bulbous, infectious hyphae in the first-invaded plant cell, and, subsequently, grows into neighboring cells, presumably through the plasmodesmata (Kankanala *et al.*, 2007).

In *M. oryzae*, six peroxidase genes have been functionally characterized. Studies have provided evidence that both balancing the intracellular level of ROS and efficient removal of extracellular ROS are pivotal for early phase host infection. Genetic analysis of NADPH oxidase genes, *NOX1* and *NOX2*,

suggests that regulation of intracellular ROS is required for appressorium maturation and penetration peg formation (Egan *et al.*, 2007). The deletion mutant of a glutathione peroxidase gene, *HYR1*, is less tolerant to ROS and produces smaller lesions on rice plants (Huang *et al.*, 2011). The role of other putative peroxidase genes in antioxidant defense is unknown.

Mutants lacking the secreted large subunit catalase, *CATB*, are less pathogenic due to their involvement in strengthening the fungal cell wall rather than detoxifying host-derived H_2O_2 (Skamnioti *et al.*, 2007). Deletion of the catalase peroxidase gene, *CPXB*, renders the mutant sensitive to exogenous H_2O_2, but it does not impair pathogenicity (Tanabe *et al.*, 2011). Finally, loss of the peroxiredoxin gene, *TPX1*, is required for pathogenicity, but not to neutralize plant-generated ROS (Fernandez and Wilson, 2014).

There is still much to learn about peroxidases and fungal pathogenicity. First, are specific peroxidases particularly important for pathogenicity? Second, what are the relationships among peroxidases, sensitivity to exogenous H_2O_2, and pathogenicity? In an attempt to answer these questions, we performed comprehensive expression and functional analyses based on reconstruction of phylogeny for 27 putative peroxidase genes in *M. oryzae*.

MATERIALS AND METHODS

I. Identification of peroxidase genes

Putative peroxidase-encoding genes were retrieved from the Fungal Peroxidase Database (fPoxDB; http://peroxidase.riceblast.snu.ac.kr/), which is a fungi-oriented peroxidase genomics platform (Choi *et al.*, 2014). The collected protein sequences were used to conduct phylogenetic analysis. The protein sequences were aligned with ClustalW in the MEGA6.0 software with default parameters (Tamura *et al.*, 2013). Phylogenetic trees were constructed using the neighbor-joining method in the MEGA6.0 software. The peroxidase gene protein structure was obtained from the InterPro database (http://www.ebi.ac.kr/interpro).

II. Fungal strains and culture conditions

Magnaporthe oryzae KJ201 was obtained from the Center for Fungal Genetic Resources (CFGR) at Seoul National University, Seoul, Korea, and used as the wild-type in this study. This strain and all generated transformants were cultured on oatmeal agar medium (50-g oatmeal per liter with 2% agar (w/v)) or V8-Juice agar medium (4% V8 Juice, pH 6.8) at 25°C under continuous fluorescent

light, cultured in complete liquid medium (0.6% yeast extract, 0.6% casamino acid, and 1% glucose) at 25°C for 3-4 days with agitation (120 rpm) for genomic DNA extraction. For RNA extraction, all materials were prepared as described previously (Park *et al.*, 2013) (Table 1). Hygromycin B-resistant and geneticin-resistant transformants generated by fungal transformation were selected on solid TB3 agar medium (0.3% yeast extract, 0.3% casamino acid, 1% glucose, 20% sucrose (w/v), and 0.8% agar) supplemented with 200 ppm hygromycin B and 800 ppm geneticin. The wild-type and transformants were cultured on complete agar medium (CM), minimal agar medium (MM), C starvation, and N starvation medium to observe growth and colony characteristics (Talbot *et al.*, 1997). Cell wall biogenesis was examined by imposing stress conditions under 200 ppm Congo Red (CR, Aldrich, 860956) supplementation in CM agar medium. Oxidative stress conditions were elicited in CM agar medium, and amended to final concentrations of 2.5, 5, and 10 mM H_2O_2.

III. Analysis of transcript levels

Quantitative real-time RT-PCR (qRT-PCR) was employed to measure transcript levels. Total RNA samples and first-strand cDNA were prepared as described previously (Park *et al.*, 2013). qRT-PCR followed Park *et al.* (Park *et al.*, 2013) using each primer pair listed in Table 2. All reactions were performed with more

than two biological and three experimental replicates. The *β-tubulin* gene was used as the internal control for normalization. All amplification curves were analyzed with a normalized reporter threshold of 0.1 to obtain the threshold cycle (Ct) values. The comparative ΔΔCt method was applied to evaluate relative quantities of each amplified sample product. Fold changes were calculated as $2^{-\Delta\Delta Ct}$ (Livak and Schmittgen, 2001;Park *et al.*, 2013). We applied a fold-change cutoff of ≥ 1.5 for upregulation, and ≤ 0.5 for downregulation.

IV. Targeted deletion of seven peroxidase genes and Δ*Moprx1* complementation in *M. oryzae*

Based on seven peroxidase gene sequences in the *M. oryzae* genome, the 5´ (1.2-1.5-kb) and 3´ (1.2-1.5-kb) flanking regions were amplified using primer pairs from each gene: _UF and _UR for the 5´ flanking, and _DF and _DR for the 3´ flanking regions (Table 2) from KJ201 genomic DNA. The 1.4-kb HPH marker cassette was amplified from pBCATPH (Yun, 1998) using primers HPH_F and HPH_R. These three amplicons were fused by double-joint PCR (Yu *et al.*, 2004), and the resulting mutant constructs were amplified using the nested primer pair (_UNF and _DNR; as shown in Table 2). Fungal protoplasts from wild-type KJ201 were directly transformed using the double-joint PCR

product following purification using the standard polyethylene glycol method. Putative gene deletion mutants were screened, and the candidate gene deletion mutants were subsequently purified by single conidia isolation. Southern blot analysis was performed to confirm deletion mutants (Figure 4).

ΔMoprx1 complementation was achieved by amplifying a 3.6-kb fragment containing the *MoPRX1* open reading frame (ORF), and a 1.3-kb of the 5´ and 1.2 kb of the 3´ flanking regions from wild-type genomic DNA using the *MoPRX1*_UF and *MoPRX1*_DR primers. Geneticin resistance fragment was amplified from PII99(Chi *et al.*, 2009a) vector plasmid with primers HPH_F (2.1kb) and HPH_R (2.1kb) (Table 2). The purified 3.6-kb complementation construct was co-transformed with the geneticin fragment into *ΔMoprx1* protoplasts. Putative complemented transformants were selected on TB3 plates amended with 800 ppm geneticin. After genetic purification by single conidium isolation, complements were confirmed by *MoPRX1* gene expression through RT-PCR (Figure 4a).

V. Nucleic acids manipulation and Southern blotting

Most molecular biology-related techniques, including clone preparation, plasmid DNA, restriction enzyme digestion, and Southern blot analysis, were

performed as described previously (Park *et al.*, 2003). Genomic DNA and total RNA were extracted following Park *et al*. (Park *et al.*, 2003) and Park *et al.* (Park *et al.*, 2013) respectively. For PCR screening of generated transformants, genomic DNA was extracted using a rapid and safe DNA extraction method (Chi *et al.*, 2009b).

VI. *In vitro* growth assays, monitoring of infectious growth, and pathogenicity assays

Vegetative growth was measured on CM and MM agar plates at 7 and 12 days post incubation (dpi) with three replicates. Melanization, conidiation, conidial size, conidial germination, and infection assays on rice sheath cells, onion epidermis, and rice seedlings were conducted as described previously (Koga *et al.*, 2004; Kim *et al.*, 2009). For pathogenicity test,10 ml conidial suspension (5×10^4 spores/ml) containing Tween 20 (250 ppm) was used to spray onto susceptible 3-week-old rice seedlings (*Oryza sativa* cv.Nakdongbyeo). Disease severity was measured at 7 dpi and disease leaf area (DLA) was measured for more accurate evaluation. The disease area and healthy leaf area were measured using the Image J software (http://imagej.nih.gov/ij/) from equal areas of infected leaves of each strain. All experiments were replicated a minimum of

three times. The rate of appressorium formation was measured as the percentage of germinated conidia that developed appressoria at 8, 16 and 24 hours each after incubation. These assays were performed with three replicates in three independent experiments.

For conidiation, conidia was collected from 7-days-old V8 juice agar plates with 5ml sterilized distilled water and measured by counting the number of asexual spores within 10μl conidia suspension onto hematocytometer under a microscope. For microscopic observation of invasive growth on rice tissue, excised rice sheath of Nakdongbyeo were prepared by standard process (Koga *et al.*, 2004). Conidia suspension was injected in excised rice sheaths and incubated in moistened box for 24 and 48 hours at room temperature. After incubation, the infected rice sheaths were trimmed to remove chlorophyll enriched plant parts. Remaining epidermal layers of mid vein (three to four cell layers thick) were used for microscopic experiment. For infiltration, a wound inoculation experiment was performed by cutting leaves from plants, which were subsequently wounded with a needle tip prior to inoculation with 40-μl conidial suspension; the same concentration used in spray inoculation. Leaves were placed in a moist box and incubated in a growth chamber. Photographs were taken at 5 dpi. For rice root inoculation, mycelial blocks were plugged on

the root surface of seedlings placed on water agar and incubated in a sealed growth chamber. Lesions were observed and photographs were taken at 5 dpi.

VII. Staining of H_2O_2 accumulation in host cells

DAB (3,3´ diaminobenzidine, Sigma, D-8001) staining was conducted as described previously (Chi *et al.*, 2009a). Excised sheath samples were incubated in 1 mg/ml DAB solution at room temperature for 8 h, and destained with clearing solution (ethanol: acetic acid = 94:4, v/v) for 1 h. H_2DCFDA staining was also performed with excised rice sheaths following Huang *et al*. (Huang *et al.*, 2011). Inoculated excised rice sheaths were incubated for 1 h in 5-20 mM H_2DCFDA dissolved in DMSO at room temperature, washed with 0.1 mM KCl, 0.1 mM $CaCl_2$ (pH 6.0), and maintained at room temperature for 1 h before observation. Fluorescence and DIC micrographs were generated using a Zesis Axio Imager AI fluorescence microscope (Carl Zeiss, Oberkochen, Germany). UV light and GFP filter were used to detect phenolic compounds and ROS signals after staining with H_2DCFDA.

VIII. Yeast strain and complementation assays

The *S. cerevisiae* strains YBL064c (*ΔPrx1*) and BY4742 (wild-type) were

obtained from EUROSCARF (http://web.uni-frankfurt.de/fb15/ mikro/euroscarf/), and maintained on YPD medium. The *MoPRX1* ORF was amplified from first-strand cDNAs of the wild-type with primers *MoPRX1*_ORF_F_HindIII and *Moprx1*_ORF_R_XbaI (Table 2), and cloned into the *Hind*III and *Xba*I sites of pYES2 (Invitrogen, Carlsbad, CA, USA). The isolated plasmid pSY259 was transformed into the yeast strain YBL064c (Δ*Prx1*), using the lithium acetate method (Shiestl and Gietz, 1989). Ura3+ transformants were isolated, and the presence of the *MoPRX1* ORF in the transformants was double confirmed by PCR. For complementation assays, cells were cultured overnight, diluted in phosphate-buffered saline and cells were counted using a hemocytometer to adjust the required concentration. The final concentration was adjusted to 2×10^3 cells/μl, and aliquoted in 100-μl samples for each strain. Samples were heated to 50°C for different time intervals until lethal heat shock was reached, cooled on ice, and 10-μl samples were plated on YPD agar medium. The plates were incubated at 30°C for 2 days. Cells were counted and survival rate was measured. Oxidant chemical sensitivity was also tested using 10-μl aliquot patch assays containing 10^3, 10^4, and 10^5 cells from overnight cultures, spotted on YPD agar medium supplemented with 3, 4, and 4.5 mM H_2O_2, respectively.

IX. Measurement of extracellular peroxidase and laccase activities

Extracellular enzyme activity was measured using 3-day-old CM liquid culture filtrate. The measurement was performed by following Chi *et al.* (Chi *et al.*, 2009a). Peroxidase and laccase activities were measured by combining 1 ml of reaction mixture (50 mM sodium acetate buffer, pH 5.0 and 20 mM ABTS [Sigma, A1888]) with 200-µl culture filtrate, followed by incubation for 5 min at 25°C. Absorbance was evaluated at a 420-nm wavelength using a spectrophotometer. Three independent biological experiments, with three replicates per experiment, were performed for each test. A mycelial block was placed on CM medium containing 200 ppm Congo Red agar plate for 9 dpi to measure peroxidase secretion. Laccase activity was also monitored on 0.2 mM ABTS agar plate assays with or without 0.5 mM copper sulfate at 4 dpi.

X. Cellular localization of MoPRX1::GFP

The MoPRX1::eGFP fusion construct was generated by double-joint PCR. A 2.3-kb genomic fragment, including the putative promoter and full *MoPRX1* ORF region, was amplified with primers *MoPRX1*_UF and *MoPRX1*_ORF_R_eGFP (Table 2). The *eGFP* ORF (0.7 kb) with terminator (0.3 kb) was amplified with primers eGFP_F and NC_Term_R from the SK2707

plasmid as a template. The resulting PCR products were fused by double-joint PCR (Yu *et al.*, 2004) using primers *MoPRX1*_5NF and NC_Term_NR. The eGFP fusion construct was introduced into *ΔMoprx1* by co-transformation with pII99 (Chi *et al.*, 2009a) plasmid, which carried the geneticin-resistance gene. MoPRX1::eGFP cellular localization was observed in conidia, appressoria and infectious hypha within rice cells at 48 hpi using a fluorescence microscope (Carl Zeiss Microscope Division, Oberkochen, Germany) with a GFP filter.

XI. Computational analysis

All sequence information used in this study was taken and analyzed from the online database Comparative Fungal Genomics Platform (CFGP) (Choi *et al.*, 2013), http://cfgp.snu.ac.kr/) and BLAST program provided at the National Center for Biotechnology Information, Bethesda, USA (http://www.ncbi.nlm.nih.gov/blast/) (McGinnis and Madden, 2004). Sequences were aligned by ClustalW algorithm (Thompson *et al.*, 1994).

Table 1. RNA was extracted from five selected conditions including infection-related developments (conidia, germinated conidia and appressoria) and oxidative stress treatment

Categories	**Condition**	**Conc.**	**Treated time**	**Basal medium for treatment**
Infection-related developments	Conidia			
	Germinated conidia			
	Appressoria			
	78 hpi on compatible rice			
Oxidative stress	H_2O_2	2.5 mM	4 h	CM

Note: Germinated conidia and appressoria were harvested after 4 h and 16 h, respectively, on hydrophobic surface for RNA extraction.

Table 2. Oligo sequences used in this study

Primer name	Sequence (5’ → 3’)
Knock-out constructs	
MoPRX1	
*MoPRX1*_UF	TTCCAGGGGTACTATGGCAACAA
*MoPRX1*_UR	CCTCCACTAGCTCCAGCCAAGCCA
	ATCCGGGCCCAGTTTAGGTTTAT
*MoPRX1*_DF	GTTGGTGTCGATGTCAGCTCCGGAG
	TCAATATGGCGCCGCAGCAGTAAT
*MoPRX1*_DR	GTACTCGCCTGCCCTGCCTATCTT
*MoPRX1*_UNF	GCTGCTAAAGGGATTGGCTACTCA
*MoPRX1*_DNR	ATGGTCGCCGCTATTTGCTTATG
*MoPRX1*_UF_F	ATAAACCTAAACTGGGCCCGGATT
*MoPRX1*_DF_R	ATTACTGCTGCGGCGCCATATTGA
MoCCP1	
*MoCCP1*_UF	TCTCGTTCCTGCAGATGCCGTC
*MoCCP1*_UR	CCTCCACTAGCTCCAGCCAAGCCTGAGGT
	CTCTGACTTCAGTGGTAGGT

*MoCCP1*_DF	GTTGGTGTCGATGTCAGCTCCGGAGTTGGGG AGGACT TGATGGTTAGACTTG
*MoCCP1*_DR	CAGCCTGGACTCGAGCAACAC
*MoCCP1*_UNF	GCCGGAACTTCCAGTTTGAAGACA ACTACCTA
*MoCCP1*_DNR	AAACTGAGCGAGGACTACGACGCC
*MoCCP1*_UR_F	ACCTACCACTGAAGTCAGAGACCTCA
*MoCCP1*_DF_R	CAAGTCTAACCATCAAGTCCTCCCCAA

MoAPX1

*MoAPX1*_UF	CAGTGGAGGAATCAGCAACTCTCAGC
*MoAPX1*_UR	CCTCCACTAGCTCCAGCCAAGCCCCATTG CCTTTATGCGGAAGTTCTTGT
*MoAPX1*_DF	GTTGGTGTCGATGTCAGCTCCGGAGCATGAG CGCGTTTCACAGGACTC
*MoAPX1*_DR	TGACACGCCAAGACCTACCACAGAG
*MoAPX1*_UNF	AAGGGGAAACATTGCGCAGACATCACA
*MoAPX1*_DNR	CTTGCCAGCCTATCTTGTCCAGTAGTGG
*MoAPX1*_UR_F	ACAAGAACTTCCGCATAAAGGCAATGG
*MoAPX1*_DF_R	GAGTCCTGT GAAACGCGCTCATG

MoAPX2

*MoAPX2*_UF	GCGGCTATAGAAAGATCCGGCATGAAT
*MoAPX2*_UR	CCTCCACTAGCTCCAGCCAAGCCACAG
	CAGAT TGTGTGGTGATGCAC
*MoAPX2*_DF	GTTGGTGTCGATGTCAGCTCCGGAG
	GGATGAGAA TGAGCCAAGCAGGGAATT
*MoAPX2*_DR	TCGGAGACGCCTAGCCTTCCCTA
*MoAPX2*_UNF	AGGTCTCTTAAGGCACATTTCGTGCGG
*MoAPX2*_DNR	TGCCCCTAGAACTCGTTAGTCAGTCTAGTTCG
*MoAPX2*_UR_F	GTGCATCACCACACAATCTGCTGT
*MoAPX2*_DF_R	AATTCCCTGCTTGGCTCATTCTCATCC

MoHPX1

*MoHPX1*_UF	TCGTGAGAGGTGAGGACAATAAAC
*MoHPX1*_UR	CCTCCACTAGCTCCAGCCAAGCCCTGCCA
	AAG GACGAAGGATTGAAA
*MoHPX1*_DF	GTTGGTGTCGATGTCAGCTCCGGAGACT
	GCTGTTTGAGATGTCCA
*MoHPX1*_DR	CAACACGCATGACTCCACCTACAA
*MoHPX1*_UNF	TGGCTAGACATCTGAGGTTAT

*MoHPX1*_DNR	CTGGTTCGAGGATGTTTAGTT
*MoHPX1*_UR_F	TTTCAATCCTTCGTCCTTTGGCAG
*MoHPX1*_DF_R	TGGACATCTCAAACAGCAGT

MoLDS1

*MoLDS1*_UF	GGTAAGTAACATGCTAGGCATTTGGAG TCTCG
*MoLDS1*_UR	CCTCCACTAGCTCCAGCCAAGCCGCAATG GGA ACGCCATCGTGTATT
*MoLDS1*_DF	GTTGGTGTCGATGTCAGCTCCGGAGTGA CTGTTG GTGGGATAAGACTGAATGAA
*MoLDS1*_DR	GACTGGAAAGTGCCAAGTATCCTGCTA
*MoLDS1*_UNF	GCGGTCTGATAGACCAATTAATAGCGA GGCTAAC
*MoLDS1*_DNR	ACATTCAGGGACAATGAATACGTCCCTGCAG

TPX1

*TPX1*_UF	GCGGTTGAATCTCGGACATA
*TPX1*_UR	CCTCCACTAGCTCCAGCCAAGCCAGGGTA

	TGGCTCACG AAACTAAG
*TPX1*_DF	GTTGGTGTCGATGTCAGCTCCGGAGTGTA
	GGATGAGCGACGATAGT
*TPX1*_DR	AAGTTCGTCGAGGTTTCGGA
*TPX1*_UNF	CGAATTGAAGCACGCTGAGAGGTT
*TPX1*_DNR	TTGACCTGTTCTCGCGCTTCTTTG
*TPX1*_UR_F	CTTAGTTTCGTGAGCCATACCCT
*TPX1*_DF_R	ACTATCGTCGCTCATCCTACA

Hygromycin phosphotransferase

*HPH*_F (1.4 Kb)	GGCTTGGCTGGAGCTAGTGGAGG
*HPH*_R (1.4Kb)	GTTGGTGTCGATGTCAGCTCCGGAG
*HPH*_F (2.1 Kb)	AGAAGATGATATTGAAGG
*HPH*_R (2.1Kb)	GCACAGGTACACTTGTTTAGAG
SYP_HPH_R	ATGCCTGAACTCACGCGACGTCTGTCG

GFP tagging

*MoPRX1*_ORF_R_eGFP	TCGCCCTTGCTCACCATCTCCT TGGGCAG
eGFP_F	ATGGTGAGCAAGGGCGAGGAG
NcTerm_R	ATCATCATGCAACATGCA
NcTerm_R_nested	GATGTATTAAGAGTATAGGGGTC
*MoPRX1*_ORF_F_HindIII	AAGCTTATGGCCGAAGAGCAGCGT
*MoPRX1*_ORF_R_XbaI	TCTAGACTACTCCTTGGGCAGCGG CGTA

qRT-PCR

β-Tubulin	
Tub_F	CTCCAGGGTTTCCAGATCAC
Tub_R	CCTCACCAGTGTACCAATGC
*MoAPX1*_qRT_F	CTTTCAGCCATGGTGTTTCTG
*MoAPX1*_qRT_R	ATGTCTTCCAGCTCATCGTG
*MoAPX2*_qRT_F	CAGGACTTGAAGACACTTGGG
*MoAPX2*_qRT_R	GTAACAGTGAAGGACGAGATACC

*MoAPX3*_qRT_F	ACGCCAGCATCTTTTACGAG
*MoAPX3*_qRT_R	CAAGGTCTCCAAACGTCGAG
*CPXA*_qRT_F	TGTTCCCGTTCCATTCACTC
*CPXA*_qRT_R	GATCTGTTCCGTGGTAACTCG
*CPXB*_qRT_F	TGACCTGATTGACGATGCC
*CPXB*_qRT_R	CTTGTCAGAGTTGCGGTAGG
*MoCCP1*_qRT_F	GATGGTCCTAAGCAGTACGTC
*MoCCP1*_qRT_R	CGGCAGAGAAGTCCTTGAAG
*MoCCP2*_qRT_F	ACGGGTCTGAAGCAGTTTG
*MoCCP2*_qRT_R	GAAATCCGCAAAGAACAGGTC
*MoLIP1*_qRT_F	GCGTCCCACACTTCTCAC
*MoLIP1*_qRT_R	GCTTGTCGTGGAAGTTTTCG
*MoLIP2*_qRT_F	CGTCAATGGTAACAAACTCTGC

*MoLIP2*_qRT_R	AGGAAAGCAGTCATGGAAGG
*MoLIP3*_qRT_F	CTTCACCTCTTGACTCAACCG
*MoLIP3*_qRT_R	ATGGAGGGATAAATGTCGGTG
*NOX3*_qRT_F	ATCAACACCCAGAGAAACCC
*NOX3*_qRT_R	GTACACTACATTCGGGTCATCG
*NOX2*_qRT_F	GAGAGGCAGAAGGAACTTACG
*NOX2*_qRT_R	TCCTTGACAGCATAGTTGACG
*NOX1*_qRT_F	ATTGATGGTCCCTATGGTGC
*NOX1*_qRT_R	ACCAATACCAGTTCCAATGAGG
*MoHPX1*_qRT_F	GGAAGGACTGGGTCAAGATTC
*MoHPX1*_qRT_R	TTTCCTGGGCTGTGATCTTG
*MoHPX2*_qRT_F	TTCACCTTTATCGAGTCGGC
*MoHPX2*_qRT_R	TGCTCGAAAGGAAGACGTTC

*MoHPX3*_qRT_F	CGGGAGTGGTTGAAGGTTATT
*MoHPX3*_qRT_R	CCTGCTCAAACTTGTGGAAAC
*CATA*_qRT_F	ACTTTAGCAACATCACCTCGG
*CATA*_qRT_R	GTCGGTATAGAATCTCGTGGC
*CATB*_qRT_F	CTTTCCTCTCACTTCCTCTTCC
*CATB*_qRT_R	AGTCAACTAACCCTTGGTGTG
*MoLDS1*_qRT_F	CTACAACCATCCCTTCAACCC
*MoLDS1*_qRT_R	GAGTCAAAGATCAGCCCAGG
*MoLDS2*_qRT_F	CTTTCCCTAACCACTACGCC
*MoLDS2*_qRT_R	GACCCAGACTCTCCATAATCTTC
*MoPRX1*_qRT_F	TGGATCAAGGACATCAACGAC
*MoPRX1*_qRT_R	GCGGATGGTAAAGGCAATTC
*TPX1*_qRT_F	CCCGTGGAGTGTTCGTTATTG
*TPX1*_qRT_R	CCTTAGCCTCTTCAACCTTGG

MoPRX2_qRT_F	AGCCACATCCCTTCATACATG
MoPRX2_qRT_R	GCCCAAGCCTTCATAACAAAG
MoPRX3_qRT_F	TTGTCATCGTCAGTGTTCCG
MoPRX3_qRT_R	CTTCTCGACGTAGCTCTTGAG
MoVPX1_qRT_F	TCACTCCATACCTCCCTGAG
MoVPX1_qRT_R	GTTTTCCTGGCGATGCTTG
MoCMD1_qRT_F	CTCTCGGATAAGCAGTGGG
MoCMD1_qRT_R	GTGATCTCGACAACCTCACG
HYR1_qRT_F	GACTACAAGGGCAAGGTCG
HYR1_qRT_R	GAAGCCGAGGATGGTAAAGTC

RESULTS

I. Phylogenetic analysis of peroxidase genes in *M. oryzae*

For systematic analysis of peroxidase genes in *M. oryzae*, we first investigated the evolutionary relationships among peroxidase genes in filamentous fungi by constructing a phylogenetic tree. Searching through the Fungal Peroxidase Database (fPoxDB; http://peroxidase.riceblast.snu.ac.kr/), a total of 896 peroxidase genes were identified from genomes of 35 species that included 29 fungi, 1 chromista, 3 metazoa, and 2 viridiplantae (Table 3). In *M. oryzae*, we found 27 putative peroxidase-encoding genes. Protein sizes ranged from 160 (MoPRX3) to 1171 (MoLDS2) amino acids (Table 4). SignalP (http://www.cbs.dtu.dk/services/signalP/) predicted nine of them (*MoAPX1*, *MoAPX2*, *CPXB*, *MoLIP1*, *MoLIP2*, *MoHPX1*, *MoHPX2*, *MoHPX3* and *CATB*) to contain signal peptides (Table 4). Using amino acid sequences of putative peroxidases, including 27 *M. oryzae* peroxidases, the phylogeny of these peroxidases was reconstructed. The resulting phylogenetic tree revealed that the fungal peroxidases are not explicitly divided into distinct subgroups, with most

Table 3. Peroxidase genes from 29 fungal, 3 metazoan, 2 viridiplantae and 1 chromistal genomes

Kingdom	Phylum/ Subphylum	Species name	No. of Peroxidses	Haem peroxidase						Non-haem peroxidase			
				Animal peroxidase-Cyclooxygenase superfamily	Catalase superfamily	Class I	ClassII	DyP-type peroxidase	NAD(P)H oxidase superfamily	Alkylhydroperoxidase D-like superfamily	Glutathione peroxidase	Haloperoxidase	Peroxiredoxin
Chromista	Oomycota	*Phytophthora infestans*	31	0	2	4	0	7	4	0	7	0	7
Fungi	Ascomycota	*Aspergillus fumigatus* Af293	25	3	4	3	0	4	1	2	1	0	7
		Aspergillus nidulans	25	3	4	3	0	5	1	2	1	0	6
		Blumeria graminis f.sp. *hordei*	14	2	2	3	0	0	2	0	1	0	4
		Botrytis cinerea	30	2	6	4	0	9	1	1	1	0	6
		Candida albicans SC5314	14	0	1	2	0	0	0	0	4	0	7
		*Coccidioides immitis*RS	15	3	2	3	0	0	2	1	1	0	3
		Colletotrichum graminicola M1.001	34	4	4	4	7	5	3	1	1	0	5
		Fusarium graminearum	31	4	5	5	1	5	3	2	1	0	5
		Fusarium oxysporum	45	7	6	8	1	10	3	3	1	0	6
		Histoplasma capsulatum H88	18	3	3	2	0	2	2	1	1	0	4
		Magnaporthe oryzae 70-15	27	2	2	7	3	3	3	1	1	1	4
		Mycosphaerella graminicola	42	4	3	2	2	18	2	2	1	1	7
		Neurospora crassa	20	3	3	4	0	2	2	1	1	0	4
		Podospora anserina	23	2	4	3	1	5	3	1	1	0	3
		Saccharomyces cerevisiae S288C	11	0	2	1	0	0	0	0	3	0	5
		*Schizosaccharomyces pombe*132	5	0	1	0	0	0	0	0	1	0	3
	Basidiomycota	*Cryptococcus neoformans* var. *grubii* H99	14	0	4	2	0	0	0	0	3	0	5
		Heterobasidion irregulare TC 32-1	32	2	3	5	7	6	2	2	0	0	5
		Laccaria bicolor	23	2	1	2	1	7	2	1	1	0	6
		Melampsora larici-populina 98AG31	39	3	6	2	0	18	5	1	1	0	3
		Phanerochaete chrysosporium	39	3	5	1	16	3	2	1	1	0	7
		Puccinia graminis f. sp. *tritici*	24	0	4	2	0	12	2	0	1	0	3
		Serpula lacrymans S7.3	19	2	4	1	0	3	2	0	1	0	6
		Ustilago maydis 521	14	1	0	3	0	3	0	1	1	0	5
	Blastocladiomycota	*Allomyces macrogynus*	21	0	0	4	0	0	7	0	4	0	6
	Chytridiomycota	*Batrachochytrium dendrobatidis* JAM81	11	0	3	2	0	0	1	0	1	0	4
	Microsporidia	*Encephalitozoon cuniculi*	2	0	0	0	0	0	0	0	1	0	1
	Zygomycota	*Phycomyces blakesleeanus*	14	0	2	2	0	0	0	0	2	0	8
		Rhizopus oryzae	19	0	4	3	0	2	0	0	3	0	7
Metazoa	Arthropoda	*Dorosophila melanogaster*	20	0	2	0	0	0	2	0	4	0	12
	Chordata	*Homo sapiens*	53	0	1	0	0	0	19	0	13	0	20
	Nematoda	*Caenorhabditis elegans*	16	0	3	0	0	0	2	0	7	0	4
Viridiplantae	Streptophyta	*Arabidopsis thaliana*	63	3	7	18	0	0	14	0	9	0	12
		Oryza sativa (japonica cultivar-group)	63	4	6	18	0	0	17	0	7	0	11
		Total	896	62	109	123	39	129	109	24	88	2	211

Table 4. Predicted peroxidase encoded genes in *Magnaporthe oryzae*

	Class	Type	Locus	Protein Length	Signal peptide	Annotation
Haem	Class I peroxidase	Hybrid Ascorbate-Cytochrome C peroxidase	MGG_00461	476		hypothetical protein, *MoAPX1*
			MGG_08200	804	V	hypothetical protein, *MoAPX2*
			MGG_09398	548	V	hypothetical protein, *MoAPX3*
		Catalase peroxidase	MGG_04337	750		catalase-peroxidase 1, *CPXA*
			MGG_09834	786	V	catalase-peroxidase 2, *CPXB*
		Cytochrome C peroxidase	MGG_04545	362		cytochrome c peroxidase, *MoCCP1*
			MGG_10368	300		cytochrome c peroxidase, *MoCCP2*
	Class II peroxidase	Other class II peroxidase	MGG_07790	474	V	ligninase H2, *MoLIP1*
			MGG_10877	264	V	hypothetical protein, *MoLIP2*
			MGG_14940	428		ligninase C, *MoLIP3*
	NAD(P)H oxidase superfamily	NADP(H) oxidase	MGG_00750	553		cytochrome b-245 heavychain subunit beta, *NOX1*
			MGG_06559	582		cytochrome b-245 heavychain subunit beta, *NOX2*
			MGG_08299	849		hypothetical protein, *NOX3*
	DyP-type peroxidase	Haloperoxidase (haem)	MGG_16840	242	V	hypothetical protein, *MoHPX1*
			MGG_07574	257	V	hypothetical protein, *MoHPX2*
			MGG_07871	241	V	hypothetical protein, *MoHPX3*
	Catalase superfamily	Catalase	MGG_10061	743		catalase-1, *CATA*
			MGG_06442	715	V	catalase-3, *CATB*
	Animal peroxidase	Linoleate diol synthase (PGHS like)	MGG_10859	1153		heme peroxidase, *MoLDS1*
			MGG_13239	1171		linoleate diol synthase, *MoLDS2*
Non haem	Peroxiredoxin	1-Cysteine peroxiredoxin	MGG_08256	224		mitochondrial peroxiredoxin PRX1, *MoPRX1*
		Atypical 2-Cysteine peroxiredoxin (type Q, BCP)	MGG_07503	314		thioredoxin peroxidase, *TPX1*
		Atypical 2-Cysteine peroxiredoxin (type II &V)	MGG_00860	184		AphC/TSA family protein, *MoPRX2*
			MGG_02710	168		peroxiredoxin type-2, *MoPRX3*
	Haloperoxidase	Vanadium chloroperoxidase	MGG_02210	595		vanadium chloroperoxidase, *MoVPX1*
	Alkyhydroperoxidase D-like superfamily	Carboxymuconolactone decarboxylase (no peroxidase activity)	MGG_01347	243		4-carboxymuconolactone decarboxylase, *MoCMD1*
	Glutathione peroxidase	Fungi-Bacteria glutathione peroxidase	MGG_07460	172		peroxiredoxin HYR1, *HYR1*

Figure 1.


MGG 08256T0 (MoPRX1) Magnaporthe oryzae 70-15
GLRG 07076T0 Colletotrichum graminicola M1.001
NCU06331T0 Neurospora crassa
Pa 5 4690 Podospora anserina
FGSG 07536T0 Fusarium graminearum
FOXG 15430T0 Fusarium oxysporum f. sp. lycopersici
BC1G 00059 Botrytis cinerea
estExt Genewise1Plus.C chr 41173 Mycosphaerella graminicola
bgh02344 polypeptide Blumeria graminis f. sp. hordei DH14
ANID 10223 Aspergillus nidulans FGSC A4
Afu4g08580 Aspergillus fumigatus Af293
HCEG 00543 Histoplasma capsulatum H88
CIMG 08865.2 Coccidioides immitis
estExt fgenesh1 pm.C chr 10340 Mycosphaerella graminicola
ANID 03973 Aspergillus nidulans FGSC A4
Afu8g07130 Aspergillus fumigatus Af293
BC1G 06262 Botrytis cinerea
PGTG 17942 Puccinia graminis f. sp. tritici
EuGene.00810042 Melampsora larici-populina 98AG31
UM06404.1 Ustilago maydis 521
fgenesh1 pm.C scaffold 2000052 Phanerochaete chrysosporium
estExt Genewise1 human.C 40887 Laccaria bicolor
fgenesh1 kg.15 # 565 # 412.1 CFOT CFPN Serpula lacrymans S7.3
Hetan1.estExt fgenesh3 kg.C 40371 Heterobasidion irregulare TC 32-1
fgeneshPB pm.2 79 Phycomyces blakesleeanus
fgeneshPB pm.73 4 Phycomyces blakesleeanus
RO3G 02627 Rhizopus oryzae
CNAG 06917 Cryptococcus neoformans serotype A
estExt Genewise1Plus.C 1000001 Batrachochytrium dendrobatidis JAM81
orf19.5180 Candida albicans SC5314
YBL064C Saccharomyces cerevisiae S288C
Afu5g15070 Aspergillus fumigatus Af293
e gwh2.7.586.1 Phanerochaete chrysosporium
AT1G48130.1 Arabidopsis thaliana
LOC Os07g44430.1 Oryza sativa
LOC Os07g44440.1 Oryza sativa
FBpp0077368 Drosophila melanogaster
ENSP00000342026 Homo sapiens
FBpp0087354 Drosophila melanogaster
FBpp0087356 Drosophila melanogaster
FBpp0087406 Drosophila melanogaster
Y38C1AA.11 Caenorhabditis elegans
1-cystein peroxiredoxin
FGSG 03180T0 Fusarium graminearum
FOXG 10111T0 Fusarium oxysporum f. sp. lycopersici
GLRG 10121T0 Colletotrichum graminicola M1.001
estExt fgenesh1 pg.C 90169 Serpula lacrymans S7.3
estExt Genewise1 human.C 200095 Laccaria bicolor
fgenesh1 pg.C scaffold 19000036 Phanerochaete chrysosporium
estExt fgenesh1 pm.C 110048 Heterobasidion irregulare TC 32-1
estExt Genewise1.C 20977 Phycomyces blakesleeanus
RO3G 02462 Rhizopus oryzae
RO3G 12289 Rhizopus oryzae
RO3G 12682 Rhizopus oryzae
AMAG 01034T0 Allomyces macrogynus
AMAG 02542T0 Allomyces macrogynus
PITG 15492 Phytophthora infestans
FBpp0073594 Drosophila melanogaster
FBpp0073595 Drosophila melanogaster
F09E5.15a Caenorhabditis elegans
F09E5.15b Caenorhabditis elegans
ENSP00000262746 Homo sapiens
ENSP00000361152 Homo sapiens
ENSP00000415124 Homo sapiens
ENSP00000389047 Homo sapiens
ENSP00000407034 Homo sapiens
ENSP00000301522 Homo sapiens
ENSP00000334063 Homo sapiens
ENSP00000408139 Homo sapiens
PITG 15504 Phytophthora infestans
FBpp0072852 Drosophila melanogaster
FBpp0072853 Drosophila melanogaster
YDR453C Saccharomyces cerevisiae S288C
YML028W Saccharomyces cerevisiae S288C
orf19.7398.1 Candida albicans SC5314
orf19.7417 Candida albicans SC5314
SPCC576.03c Schizosaccharomyces pombe
R07E5.2 Caenorhabditis elegans
ENSP00000298510 Homo sapiens
ENSP00000349432 Homo sapiens
estExt Genewise1Plus.C 60058 Batrachochytrium dendrobatidis JAM81
FBpp0082927 Drosophila melanogaster
FBpp0075397 Drosophila melanogaster
PITG 00850 Phytophthora infestans
GP3.023210 Batrachochytrium dendrobatidis JAM81
AMAG 07809T0 Allomyces macrogynus
AMAG 09686T0 Allomyces macrogynus
estExt Genewise1.C 90160 Phycomyces blakesleeanus
RO3G 15723 Rhizopus oryzae
AT3G11630.1 Arabidopsis thaliana
AT5G06290.1 Arabidopsis thaliana
LOC Os04g33970.1 Oryza sativa
LOC Os02g33450.1 Oryza sativa
LOC Os02g33450.2 Oryza sativa
CNAG 03482 Cryptococcus neoformans serotype A
PITG 00986 Phytophthora infestans
ENSP00000368635 Homo sapiens
ENSP00000368646 Homo sapiens
ENSP00000368654 Homo sapiens
ENSP00000404888 Homo sapiens
ENSP00000413736 Homo sapiens
CAD26263.1 Encephalitozoon cuniculi
ENSP00000408905 Homo sapiens
LOC Os07g49400.4 Oryza sativa
ENSP00000361150 Homo sapiens
MGG 07503T0 (TPX1) Magnaporthe oryzae 70-15
FGSG 10296T0 Fusarium graminearum
FOXG 05110T0 Fusarium oxysporum f. sp. lycopersici
GLRG 07483T0 Colletotrichum graminicola M1.001
ANID 04301 Aspergillus nidulans FGSC A4
BC1G 07040 Botrytis cinerea
estExt fgenesh1 kg.C chr 120198 Mycosphaerella graminicola
NCU11657T0 Neurospora crassa
CIMG 00966.2 Coccidioides immitis
HCEG 01271 Histoplasma capsulatum H88
bgh04299 polypeptide Blumeria graminis f. sp. hordei DH14
Afu4g05910 Aspergillus fumigatus Af293
Atypical 2-cystein peroxiredoxin
PGTG 18343 Puccinia graminis f. sp. tritici
fgenesh2 pg.25 # 19 Melampsora larici-populina 98AG31
UM04851.1 Ustilago maydis 521
e gwh2.12.297.1 Phanerochaete chrysosporium
estExt Genewise1 worm.C 80203 Laccaria bicolor
estExt fgenesh1 kg.C 150466 Serpula lacrymans S7.3
Hetan1 fgenesh2 pg.C scaffold 13000248 Heterobasidion irregulare TC 32-1
CNAG 02854 Cryptococcus neoformans serotype A
AMAG 09016T0 Allomyces macrogynus
AMAG 12030T0 Allomyces macrogynus
YIL010W Saccharomyces cerevisiae S288C
orf19.5417 Candida albicans SC5314
SPBC1773.02c Schizosaccharomyces pombe
PITG 00585 Phytophthora infestans
PITG 20585 Phytophthora infestans
UM03211.1 Ustilago maydis 521
fgenesh1 pg.C scaffold 12000051 Phanerochaete chrysosporium
estExt fgenesh1 kg.C 80343 Serpula lacrymans S7.3
eu2.Lbscf0003g06110 Laccaria bicolor
Hetan1.estExt Genewise1Plus.C 70718 Heterobasidion irregulare TC 32-1
gw1.2.829.1 Phycomyces blakesleeanus
AT3G26060.1 Arabidopsis thaliana
AT3G26060.2 Arabidopsis thaliana
LOC Os06g09610.1 Oryza sativa
LOC Os06g09610.2 Oryza sativa
Afu5g02300 Aspergillus fumigatus Af293

Figure 1. (Continued)

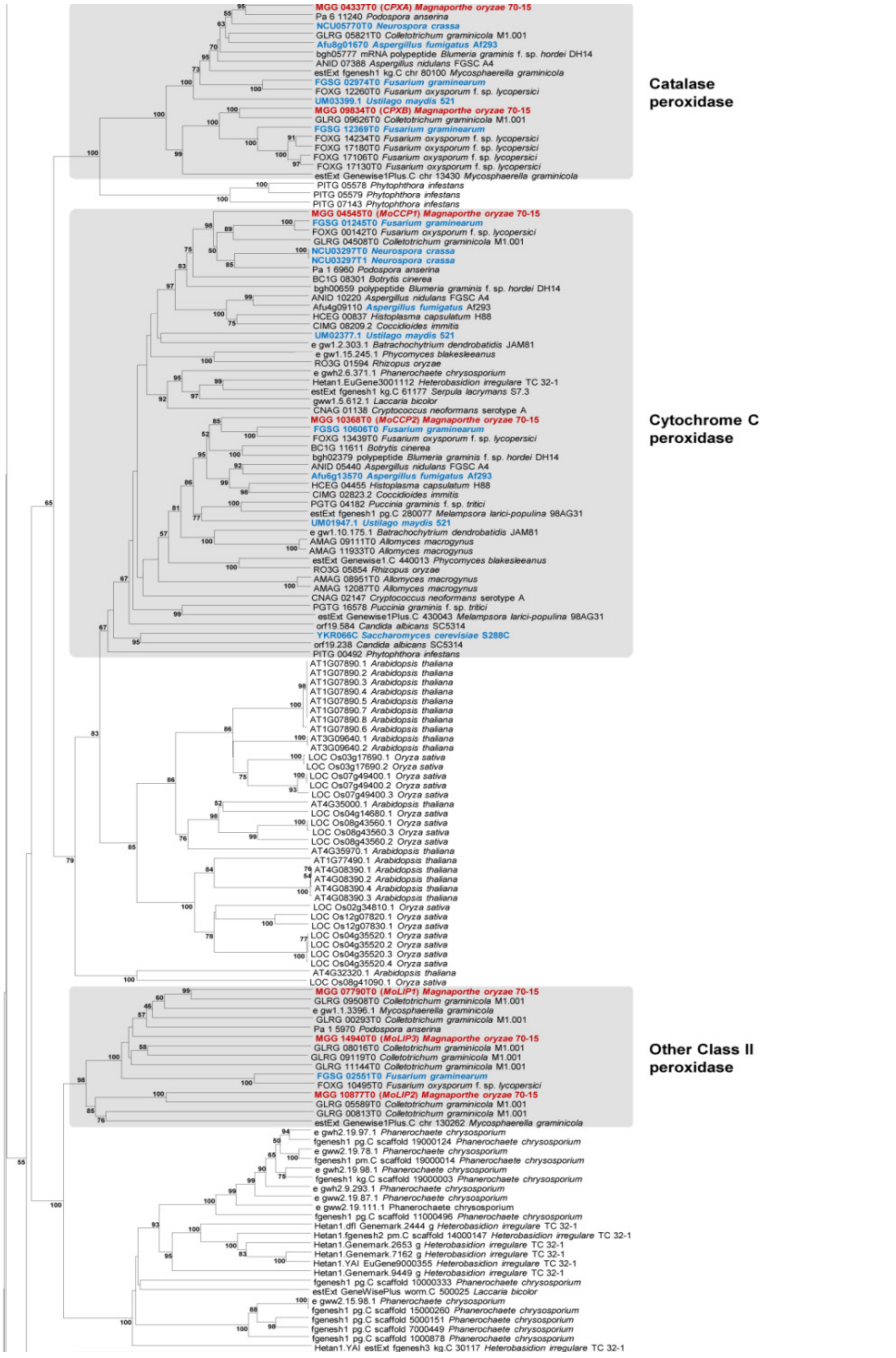

Figure 1. (Continued)

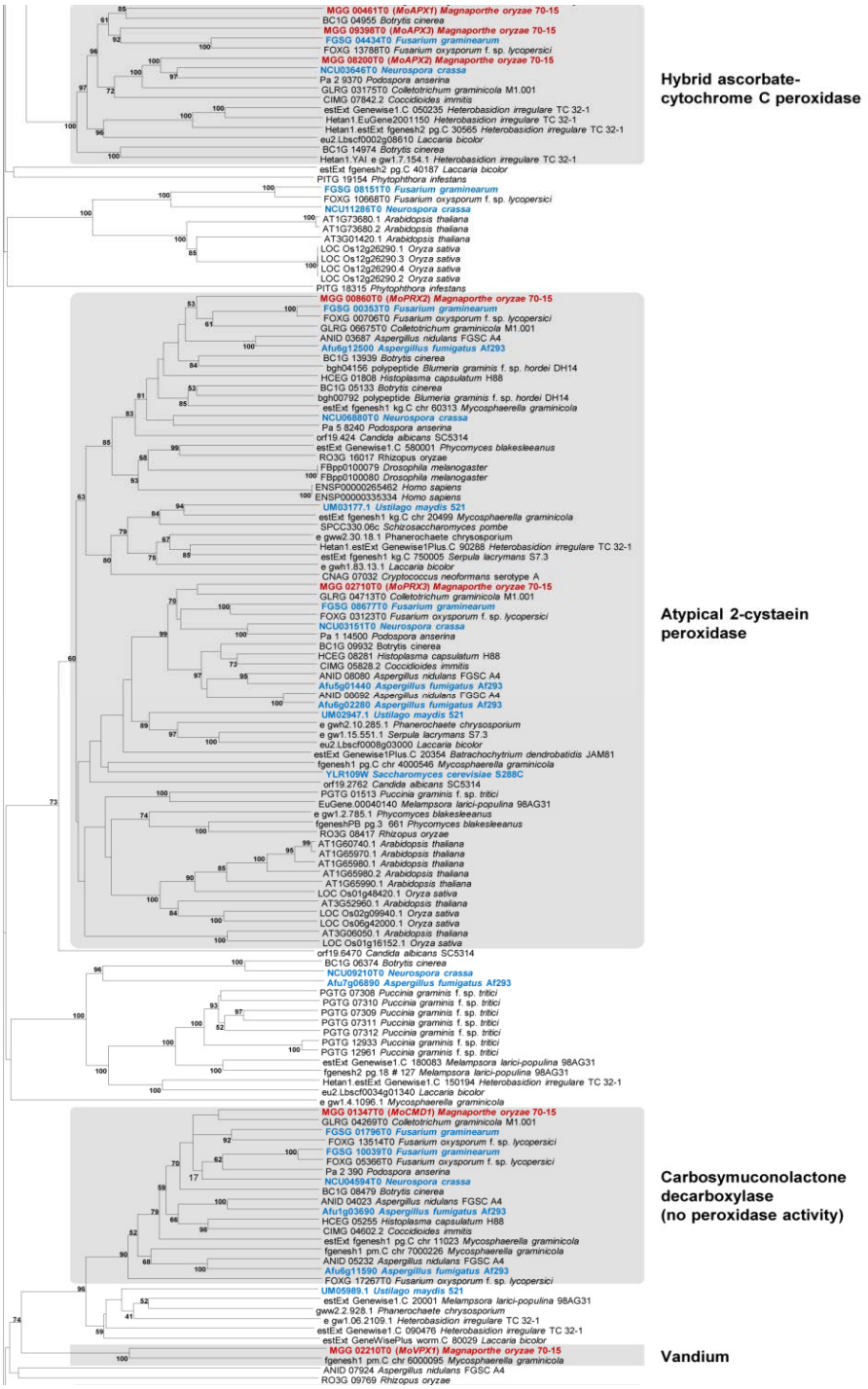

Figure 1. (Continued)

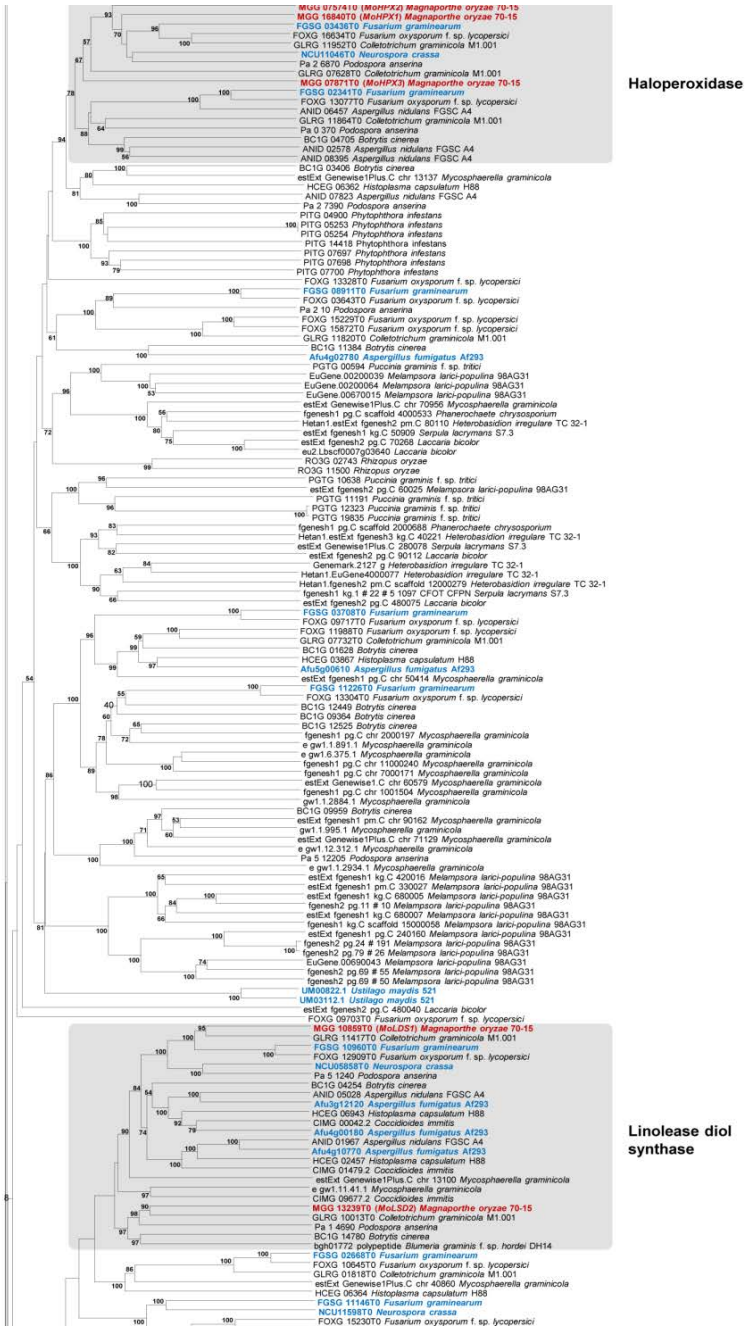

Figure 1. (Continued)

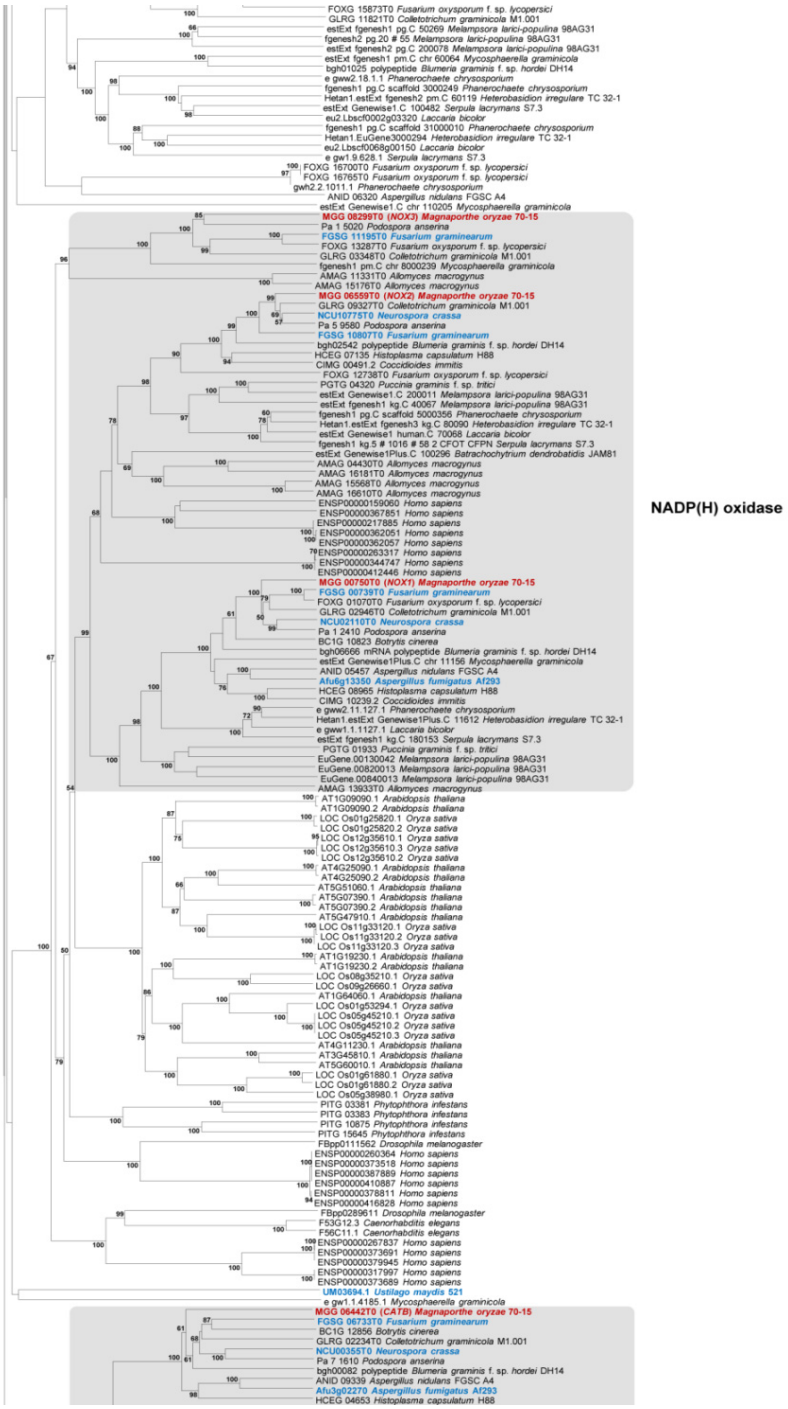

Figure 1. (Continued)

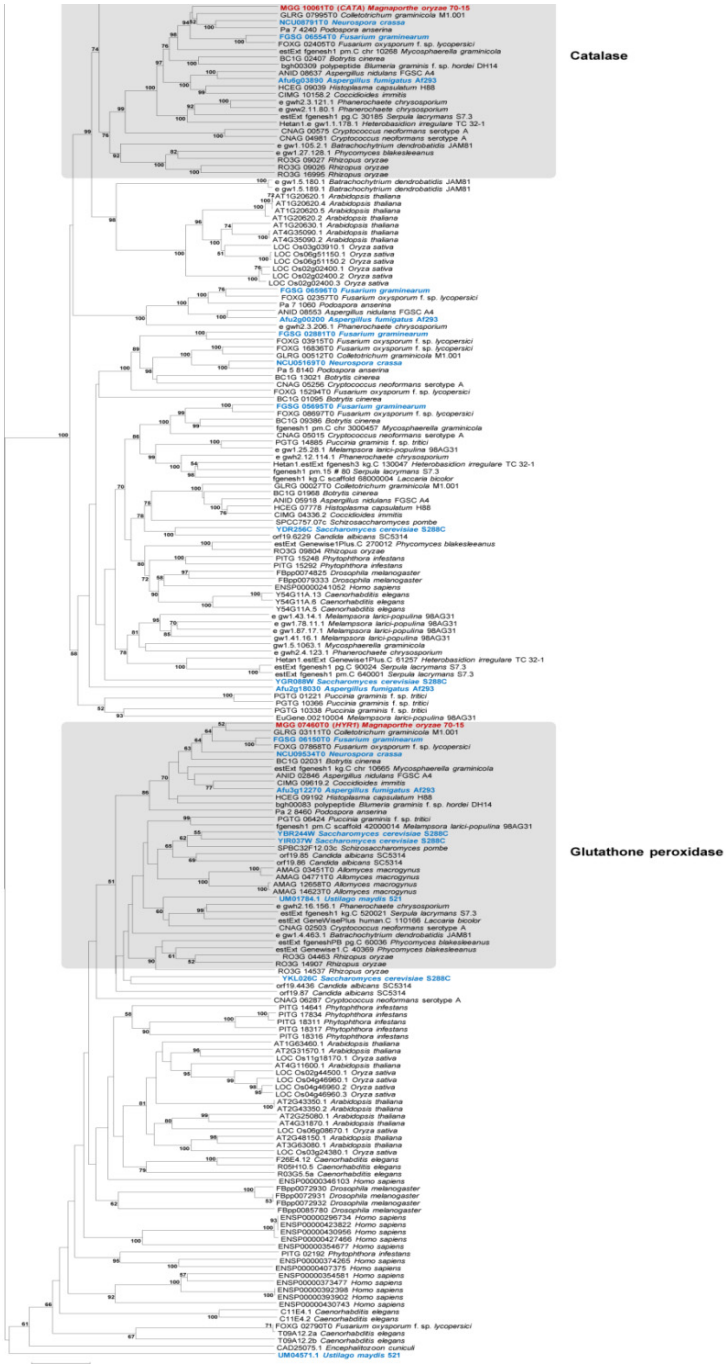

Figure 1. Phylogenetic analysis of peroxidase genes in 29 fungal, 1 chromista, 3 metazoa, and 2 viridiplantae genomes (List shown in Table 1). A neighbor-joining tree was constructed based on the amino acid sequences of all of the peroxidase genes. The numbers at the nodes indicate bootstrap values (%) in 10,000 bootstrap replicates; only nodes supported by 50 bootstraps or more are shown. Gray boxes are the phylogenetic positions of 27 Magnaporthe oryzae peroxidase genes. Red and blue bold letters denote *M. oryzae* and five selected fungal species, respectively.

nodes associated with subgroup branching and supported by low bootstrap values (Figure 1). A few peroxidases sharing domain architecture were clustered into clades. To focus our analysis on fungal peroxidases, we selected six representative fungi that included three plant pathogenic fungi (*M. oryzae*, *Fusarium graminearum*, *Ustilago maydis*), one human pathogenic fungus (*Aspergillus fumigatus*), and two saprophytic fungi (*Neurospora crassa* and *Saccharomyces cerevisiae*). Phylogenetic analysis with selected fungal species placed 27 *M. oryzae* peroxidase genes into 15 clades (Figure 2). Among the 27 peroxidase genes in *M. oryzae*, 16 genes (*MoAPX3*, *CPXA*, *CPXB*, *MoCCP1*, *MoCCP2*, *NOX1*, *NOX2*, *CATB*, *CATA*, *MoLDS1*, *MoLDS2*, *MoPRX1*, *TPX1*, *MoPRX2*, *MoCMD1* and *HYR1*) were conserved in Ascomycota (Table 5).

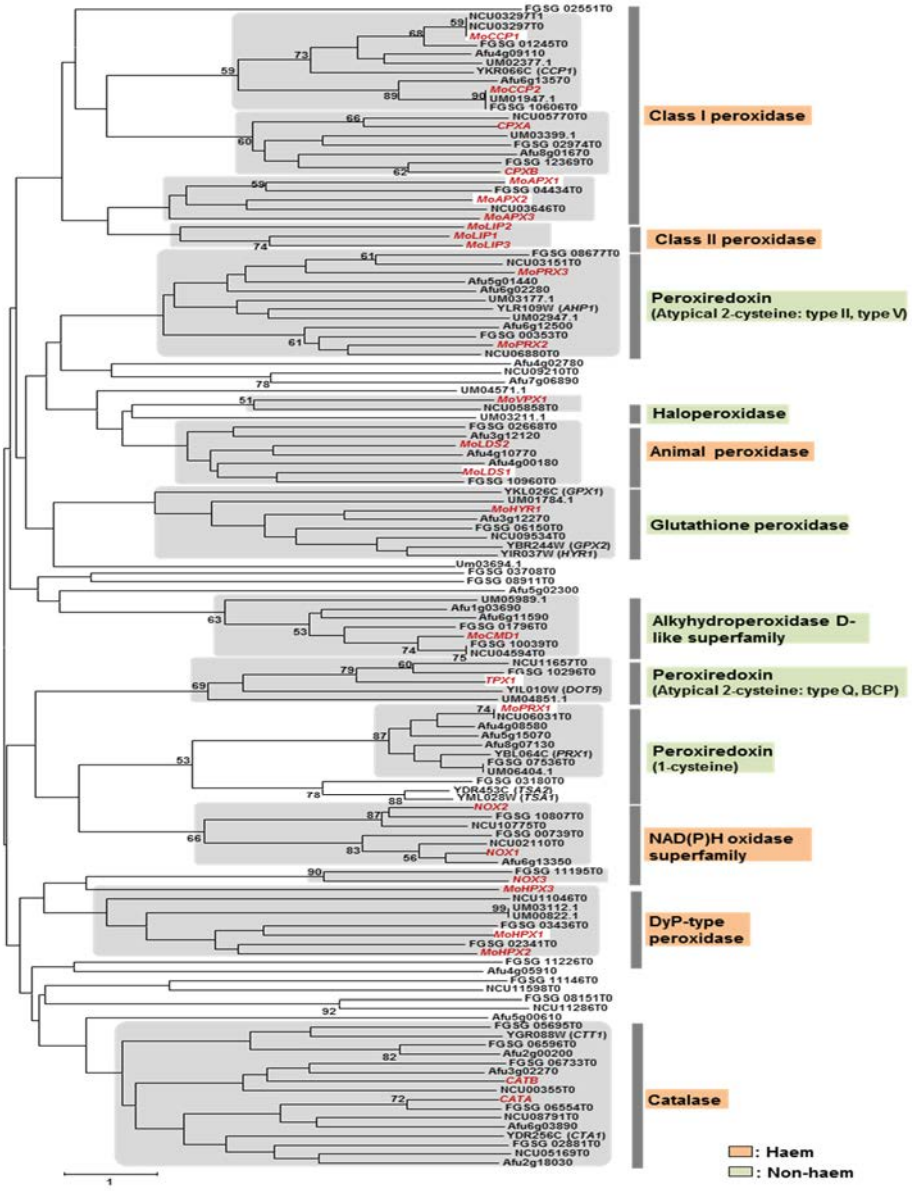

Figure 2. Phylogenetic analysis of putative peroxidase genes in six selected fungi.

Figure 2. (continued)

A neighbor-joining tree was constructed based on the amino acid sequences of representative fungal peroxidase genes. Numbers at nodes represent bootstrap confidence values, or percentage of clade occurrence in 2,000 bootstrap replicates; only nodes supported by > 50% bootstraps are shown. The scale bar represents the number of amino acid differences per site. Sub-clades containing *Magnaporthe oryzae* peroxidase genes are shaded, in which *M. oryzae* peroxidase genes and characterized genes from other fungi are depicted in bold red or black, respectively. Seven *M. oryzae* genes selected for functional analysis are also highlighted. Abbreviations for fungal species, followed by their GenBank accession numbers, are as follows: Mo, *Magnaporthe oryzae*; Sc, *Saccharomyces cerevisiae*; Fg, *Fusarium graminearum*; Nc, *Neurospora crassa*; Um, *Ustilago maydis*; Af, *Alternaria fumigatus*.

Table 5. List of 27 putative peroxidase proteins in *Magnaporthe oryzae* and BLAST Matrix results compared to those from 35 organisms

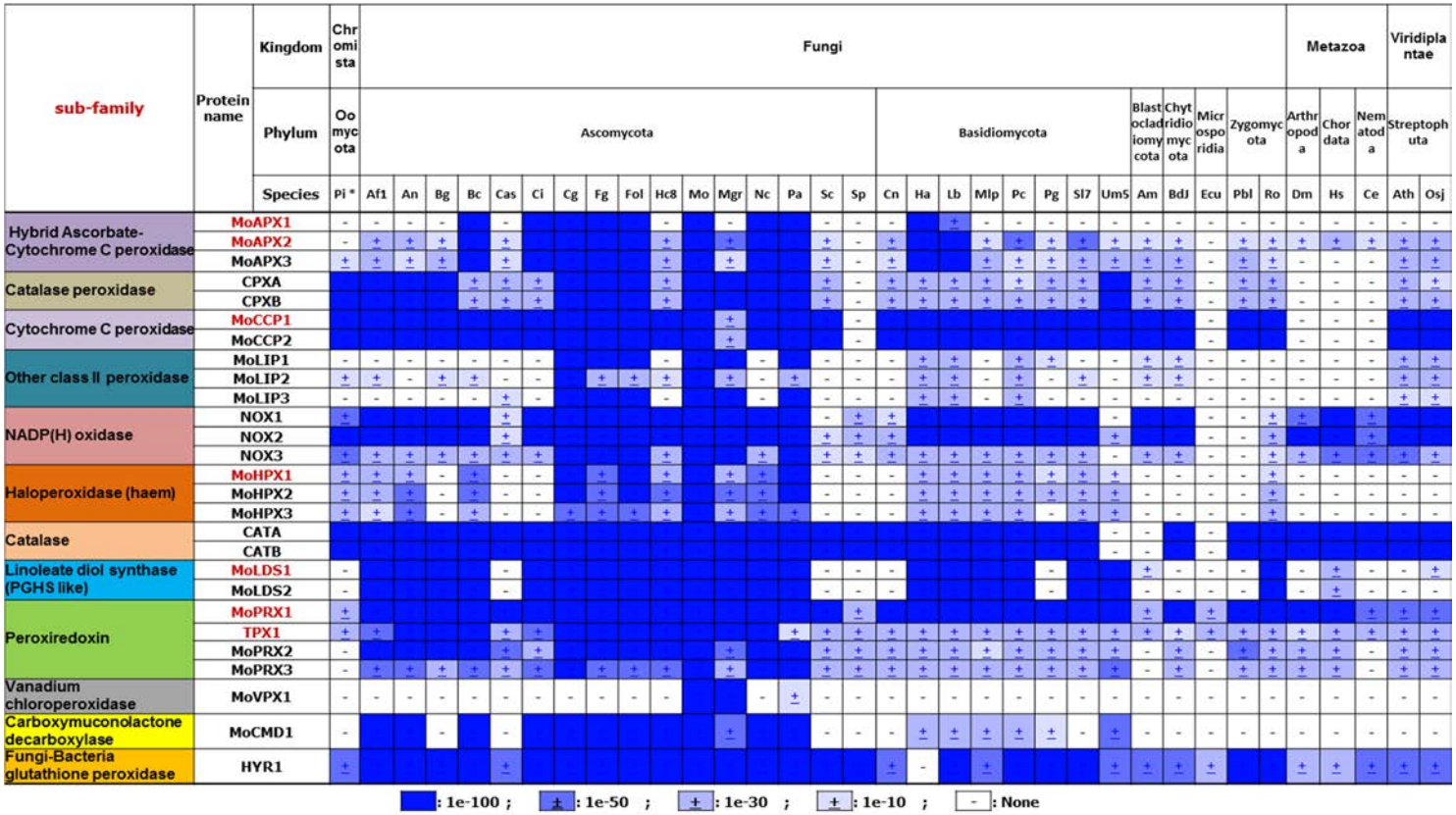

Table 5 (Continued)

*Abbreviation for fungal species and other organisms: Pi: *Phytophthora infestans*; Af1: *Aspergillus fumigatus* Af293; An: *Aspergillus nidulans*; Bg: *Blumeria graminis* f.sp. hordei; Bc: *Botrytis cinerea*; Cas: *Candida albicans* SC5314; Ci: *Coccidioides immitis*; Cg: *Colletotrichum graminicola* M1.001; Fg: *Fusarium graminearum*; Fol: *Fusarium oxysporum*; Hc8: *Histoplasma capsulatum* H88; Mo: *Magnaporthe oryzae* 70-15; Mgr: *Mycosphaerella graminicola*; Nc: *Neurospora crassa*; Pa: *Podospora anserina*; Sc: *Saccharomyces cerevisiae* S288C; Sp: *Schizosaccharomyces pombe*; Cn: *Cryptococcus neoformans* variety gatti (serotype A) ; Ha: *Heterobasidion annosum*; Lb: *Laccaria bicolor*; Mlp: *Melampsora larici-populina* 98AG31; Pc: *Phanerochaete chrysosporium*; Pg: *Puccinia graminis*; Sl7: *Serpula lacrymans* S7.3; Um5: *Ustilago maydis* 521; Am: *Allomyces macrogynus*; Bdj: *Batrachochytrium dendrobatidis* JAM81; Ec: *Encephalitozoon cuniculi*; Pbl: *Phycomyces blakesleeanus*; Ro: *Rhizopus oryzae*; Dm: *Dorosophila melanogaster*; Hs: *Homo sapiens*; Ce: *Caenorhabditis elegans*; Ath: *Arabidopsis thaliana*; Osj: *Oryza sativa* japonica.

II. Expression profiling of 27 *M. oryzae* peroxidase genes during fungal development and under oxidative stress

As a next step, we performed expression profiling of the 27 peroxidase-encoding genes using qRT-PCR during infection-related developmental stages that included conidiation, appressorium formation, and 78 h post incubation (hpi) on rice plants and under oxidative stress with 2.5 mM H_2O_2 (Figure 3). Expression analysis revealed that most of the peroxidase genes were differentially expressed under the imposed conditions. Compared to expression in mycelia, only a few genes were upregulated in developmental samples, including the conidia and appressoria. However, we found that a majority of the genes (23 genes or 85.2%) were upregulated during the infection stage at 78 hpi. Fourteen genes (51.9%), the exceptions being *MoAPX3, MoLIP2, NOX3, MoHPX2, CATA, MoPRX1, TPX1, MoVPX1 and HYR1*, were also upregulated under H_2O_2 stress conditions (Figure 3). Such an expression pattern suggested the possibility of peroxidase genes playing roles associated with ROS during plant infection.

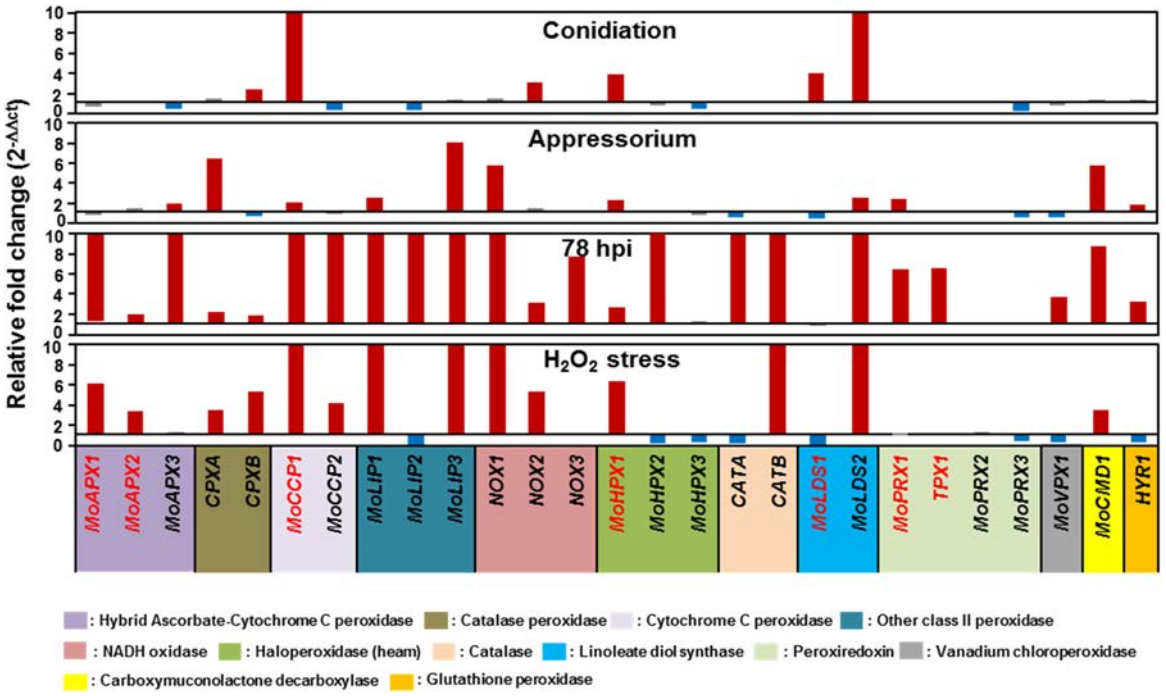

Figure 3. Expression profiling of 27 *M. oryzae* peroxidase genes during infection-related developmental stages and infection (78 hpi) on rice, and under oxidative stress.

Upregulated genes (more than 1.5-fold) are indicated by red bars and downregulated genes (less than 0.5-fold) are denoted by blue bars. The genes not showing differential expression are marked in gray.

III. Genetic analysis of peroxidase genes and fungal pathogenicity

Based on groupings from phylogenetic analysis, we prioritized seven peroxidase genes for functional analysis. We selected the genes from clades that did not contain previously characterized genes (Figure 2). The seven genes included three genes (*MoAPX1*, *MoAPX2* and *MoCCP1*) from class I peroxidase, one gene (*MoHPX1*) from Dye-type peroxidase, one gene (*MoLDS1*) from animal peroxidase, and two genes (*MoPRX1* and *TPX1*) from peroxiredoxin peroxidase (Figure 2 and Table 4). Targeted gene disruption was conducted using the KJ201 strain as wild-type to genetically assess the impact of selected putative peroxidase genes on fungal development and pathogenicity. Knockout constructs were prepared using double-joint PCR and directly used for transformation of wild-type protoplasts. The resulting hygromycin-resistant colonies were screened by PCR, and the correct gene replacement event for each targeted gene was confirmed by Southern blot analysis (Figure 4).

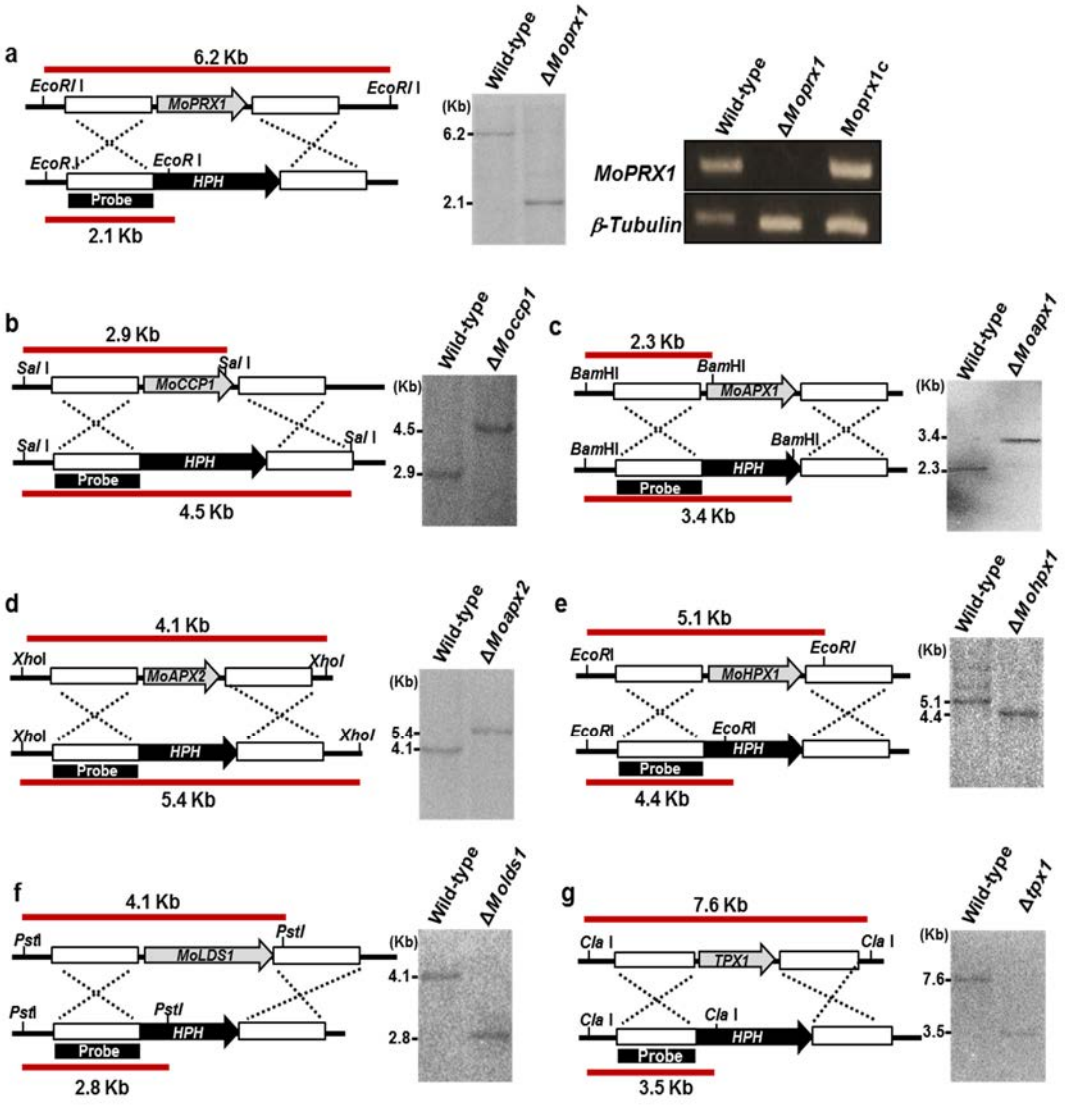

Figure 4. **Generation of deletion mutants for selected *M. oryzae* peroxidase genes.**

Figure 4. (Continued)

A total of seven knockout vectors were constructed by PCR amplification. Approximately 1.2~1.5-kb upstream and downstream flanking sequences were amplified using UF/UR and DF/DR, respectively (primer list in Table 2), and ligated with the 1.4-kb or 2.1-kb *HPH* cassette. Southern blots analysis of appropriate enzyme-digested genomic DNAs from the wild-type strain and putative gene deletion mutants. The blots were hybridized with each probe shown in Figure 4 (a-g). For the complementation of Δ*Moprx1*, putative complemented transformants were generated and tested for transcript expression of *MoPRX1* gene by RT-PCR (a).

Deletion of seven genes, one gene at a time, had minor effects on vegetative growth (Figure 5d), conidiation, conidial germination, and appressorium formation. The exception was the deletion of *TPX1*, which caused a substantial decrease in conidia production (Table 6). When we spray-inoculated 3-week-old susceptible rice seedlings with spores from wild-type and deletion mutant strains (~5×10^4 spores/ml), all seven deletion mutants (Δ*Moprx1*, Δ*Moccp1*, Δ*Moapx1*, Δ*Moapx2*, Δ*Mohpx1*, Δ*Molds1*, and Δ*tpx1)* showed reduced pathogenicity compared to the wild-type, in terms of diseased leaf area (DLA; Duncan's multiple range test, $P < 0.05$; Figure 5a., 5b.). In particular, we found that deletion of *MoPRX1* resulted in the most dramatic reduction in both number and size of lesions on rice leaves.

IV. Peroxidase activity, sensitivity to H_2O_2, and pathogenicity

The above observation that all the mutants were less pathogenic than the wild-type prompted us to explore the relationships among peroxidase activity, sensitivity to exogenous H_2O_2, and pathogenicity. Peroxidase activity was quantified by measuring absorbance of 2, 2´-azino-bis (3-ethylbenzthiazoline-6-sulphonate; ABTS) at 420 nm in culture filtrates of seven deletion mutants and the wild-type. In our assay for peroxidase activity, the deletion mutants

Table 6. Characterization of transformants including deletion mutants for seven peroxidase genes in *M. oryzae* pathogenicity-related phenotypes

Strain	Conidiation (10^5 / ml) [a]	Conidial germination (%) [b]	Appressorium formation (%) [c]
Wild-type	$55.7\pm1.5^{E\ D}$	97.7 ± 1.5^{B}	97.3 ± 1.5^{BC}
Δ*Moprx1*	42.7 ± 7.5^{B}	96.7 ± 1.2^{AB}	93.0 ± 3.6^{A}
Moprx1c	56.3 ± 1.5^{E}	94.3 ± 1.5^{A}	96.0 ± 1.0^{ABC}
Δ*Moccp1*	49.0 ± 1.0^{CD}	96.3 ± 0.6^{AB}	95.0 ± 2.6^{ABC}
Δ*Moapx1*	57.3 ± 1.2^{E}	95.7 ± 0.6^{AB}	94.7 ± 2.1^{AB}
Δ*Moapx2*	44.7 ± 2.3^{BC}	94.7 ± 1.5^{A}	97.7 ± 0.6^{BC}
Δ*Mohpx1*	50.3 ± 1.5^{D}	97.7 ± 0.6^{B}	98.3 ± 0.6^{C}
Δ*Molds1*	47.0 ± 1.0^{BCD}	95.7 ± 1.5^{AB}	95.0 ± 1.0^{ABC}
Δ*Tpx1*	10.7 ± 2.1^{A}	96.7 ± 1.5^{AB}	96.0 ± 1.0^{ABC}

[a] Conidiation was measured by counting the number of conidia collected with 5 ml of sterilized distilled water from 7-days-old V8 juice agar plate; [b] Percentage of conidial germination on hydrophobic surfaces was measured under a light microscope with three replicates; [c] Percentage of appressorium formation on hydrophobic surfaces was measured using germinated conidia using three replicates; [d] Duncan's test was used to determine significance at the 95% probability level. The same letters in a column showed no significant difference.

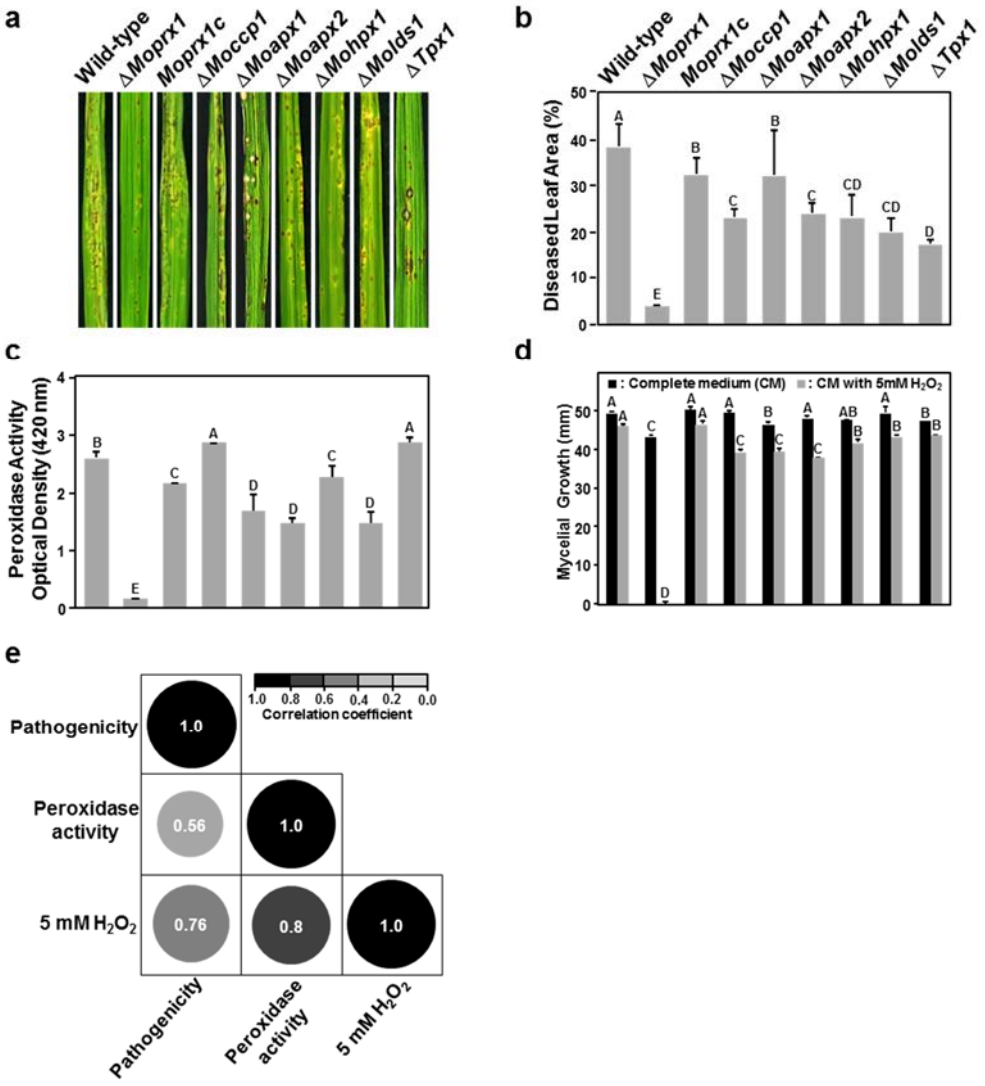

Figure 5. Pathogenicity, peroxidase activities and mycelial growth of the strains. (a) Disease symptoms on rice leaf, wild-type and seven peroxidase gene deletion mutants, including Δ*Moprx1*, Δ*Moccp1*, Δ*Moapx1*, Δ*Moapx2*,

Figure 5. (Continued)

Δ*Mohpx1*, Δ*Molds1*, and Δ*tpx1*, and one complement strain *Moprx1c*. The diseased leaves were collected at 7 dpi. (b) Disease leaf area (DLA) percentage measured using the Image J software. (c) Extracellular peroxidase activity by ABTS oxidizing assay. (d) Mycelial growth of seven deletion mutants under oxidative stress. (e) Pearson correlation coefficients among DLA from pathogenicity tests, peroxidase activity, and mycelial growth on 5 mM H_2O_2; data generated from the wild-type and seven peroxidase gene deletion mutants. Error bars represent SD of the mean of three independent experiments. Bars with the same letters are not significantly different (Duncan's multiple comparisons test, $P < 0.05$).

Δ*Moprx1*, Δ*Moapx1*, Δ*Moapx2*, Δ*Mohpx1*, and Δ*Molds1* showed reduced peroxidase activity compared to the wild-type (Figure 5c). In particular, the mutant Δ*Moprx1* lost almost all peroxidase activity. We then went on to assess the sensitivity of the deletion mutants to exogenous H_2O_2 (Figure 5d). All seven mutants were sensitive to H_2O_2, suggesting that their ability to cope with oxidative stress was compromised to varying degrees. Again, Δ*Moprx1* showed hypersensitivity to the treatment of H_2O_2. Such dramatic phenotypic defects of the Δ*Moprx1* mutant could be complemented by reintroducing a functional copy of the *MoPRX1* gene (Fig. 5 and Figure 4).

When Pearson's correlation coefficients were computed among pathogenicity (DLA), peroxidase activity, and sensitivity to H_2O_2; some of the coefficients were significant. The highest correlation was between peroxidase activity and sensitivity to H_2O_2 ($r = 0.8$). The next highest correlation was between pathogenicity and sensitivity to H_2O_2 ($r = 0.76$). The correlation between pathogenicity and peroxidase activity ($r = 0.56$) was relatively low (Figure 5e).

V. *MoPRX1* as a conserved peroxidase

In response to the general trend observed in our comprehensive approach, we investigated peroxidase-mediated fungal pathogenesis through an in-depth analysis of *MoPRX1*. MoPRX1 (224 aa) is predicted to contain two conserved domains, the thioredoxin fold domain (IPR012335) and the C-terminal peroxiredoxin domain (IPR09479). MoPRX1 is highly homologous to PRX1 in *S. cerevisiae*, which is a member of the peroxiredoxin family with 1-cysteine (proteins that contain 1 conserved cysteine directly involved in catalysis). We used a deletion mutant in the yeast gene *PRX1* to test the peroxidase activity of MoPRX1. PRX1 in *S. cerevisiae* is localized in mitochondria and is capable of removing organic hydroperoxides and H_2O_2, providing protection against oxidative stresses. Thus, the yeast mutant of *PRX1* is considerably less tolerant to H_2O_2 treatment and heat-shock is known to exacerbate this phenotype (Davidson, Whyte *et al.*, 1996). When a full-length cDNA of *MoPRX1* was introduced into a yeast strain lacking *PRX1* (YBL064c), the *MoPRX1* gene could restore the tolerance of the mutant to exogenous H_2O_2 to the wild-type level with or without heat-shock, indicating that *MoPRX1* is a functional ortholog of yeast *PRX1* (Figure 6a and 6b).

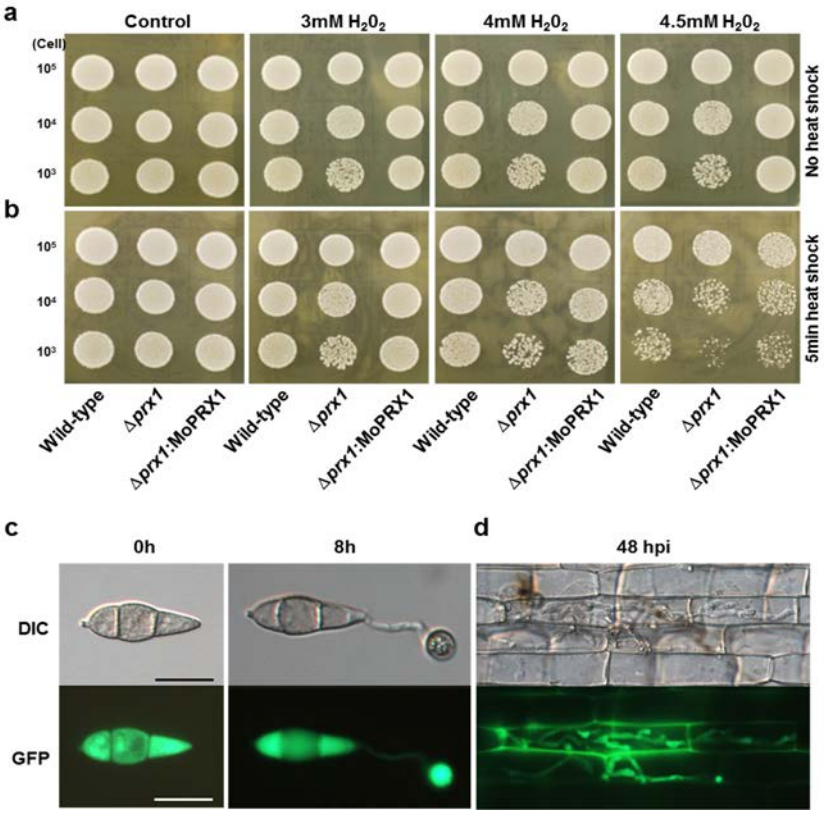

Figure 6. MoPRX1 complements *S. cerevisiae* PRX1 and localized in cytoplasm. For yeast complementation test, cells were cultured overnight, diluted in phosphate-buffered saline at a final concentration adjusted to 2×10^3 cells/μl, and aliquoted in 100-μl samples for each strain. Diluted 10 μl aliquots (10μl containing 10^3, 10^4, and 10^5 cells/μl) of wild-type (BY4742), Δ*prx1* (YBL064C), and Δ*prx1*:*MoPRX1* were exposed to 3, 4 and 4.5 mM H_2O_2 on YPD agar plates

Figure 6. (Continued)

after (a) with or (b) without 5-min heat shock at 50°C. (c) Cellular localization of MoPRX1::GFP fusion protein in a conidium and appressoria of *M. oryzae*. (d) Infectious hypha expressing MoPRX1::GFP on rice sheaths at 48 hpi. DIC images were captured using a 20-ms exposure to transmitted light with a DIC filter. Fluorescence images were captured using a 400-ms exposure to absorbed light using a GFP filter. Bar = 10 μm.

Despite functional conservation, however, MoPRX1 was not localized to mitochondria in *M. oryzae*. When a fusion construct of the *MoPRX1* promoter-*MoPRX1*-GFP was prepared and introduced into Δ*Moprx1*, a strong fluorescent signal was observed in the cytoplasm of conidia and appressoria (Figure 6c). The *PRX1* of a human pathogenic fungus, *Candida albicans*, was reported to translocate from the cytoplasm to the nucleus during hyphal transition. However, cytoplasmic localization of the protein was consistently observed, even in infectious hyphae of the rice blast fungus invading rice plant cells (Figure 6c).

VI. Roles of *MoPRX1* during early phase of host infection

To elucidate the contribution of MoPRX1, as a peroxidase, to fungal pathogenicity, we monitored wild-type and Δ*Moprx1* during the early phase of host infection using the rice sheath assay. When rice sheath cells were inoculated with fungal strains, the infection process was severely delayed in Δ*Moprx1*. In contrast to the wild-type and complementation strain (*Moprx1*c), which penetrated and colonized the first-invaded cell at 24 hpi, the mutant barely elaborated a penetration peg. At 48 hpi, infectious growth of Δ*Moprx1* was mostly confined to one to two host cells, while that of the wild-type

involved a larger number of cells involved a larger number of cells (Figure 7a). A similar pattern of delay in the early infection phase was observed in experiments using onion (*Allium cepa* L.) cells as a surrogate (Figure 8). Our observations identified a reduced number of small lesions from rice leaves spray-inoculated with Δ*Moprx1* (Figure 5a).

One possible explanation for such delayed infection is that the mutant was inherently defective in the appressorium-mediated penetration process, including penetration peg formation. To probe this possibility, conidial suspensions from Δ*Moprx1*, *Moprx1*c, and the wild-type were infiltrated into rice leaves. This allowed the fungus to gain access to plant tissues without appressorium-mediated penetration. In an infiltration experiment, Δ*Moprx1* produced smaller disease lesions compared to the wild-type and *Moprx1*c, suggesting that *MoPRX1* plays roles in the post-penetration phase (Figure 8d).

Based on our results on the peroxidase activity and H_2O_2 sensitivity of Δ*Moprx1*, we hypothesized that *MoPRX1* is involved in coping with host-derived ROS during early infection. To test this, accumulated H_2O_2 at the infection sites was examined by 3, 3´-diaminobenzidine (DAB) staining at 48 hpi, using the sheath assay. The results showed that rice sheath cells infected by wild-type and *Moprx1*c were not stained by DAB, whereas the rice cells infected with Δ*Moprx1* were strongly stained, indicating a high concentration of H_2O_2 (Figure

7b). We confirmed the accumulation of ROS using the dye 2´, 7´-dichlorodihydrofluorescein diacetate (H_2DCFDA, Life technology D-399). H_2DCFDA staining also showed fluorescence in Δ*Moprx1* infection sites, signifying ROS accumulation, but not in the wild-type or *Moprx1*c (Figure 7c). This association of ROS accumulation with the fungus lacking *MoPRX1* suggests that *MoPRX1* is implicated in direct and/or indirect detoxification of ROS.

A previous study has shown that *M. oryzae* can infect root tissue, and that this infection requires the fungus to undergo various types of programmed development, which is typical of a root-infecting pathogen (Sesma and Osbourn, 2004). The authors of that study also identified a tissue-specific virulence factor, *MgFOW1*. Therefore, our goal was to determine if *MoPRX1* is required for root infection. Our pathogenicity assay using roots of rice seedlings showed that Δ*Moprx1* cannot cause disease symptoms on root tissues, in contrast to the wild-type causing root browning (Figure 7d). This suggests that *MoPRX1* is a virulence factor required for infection of multiple tissues.

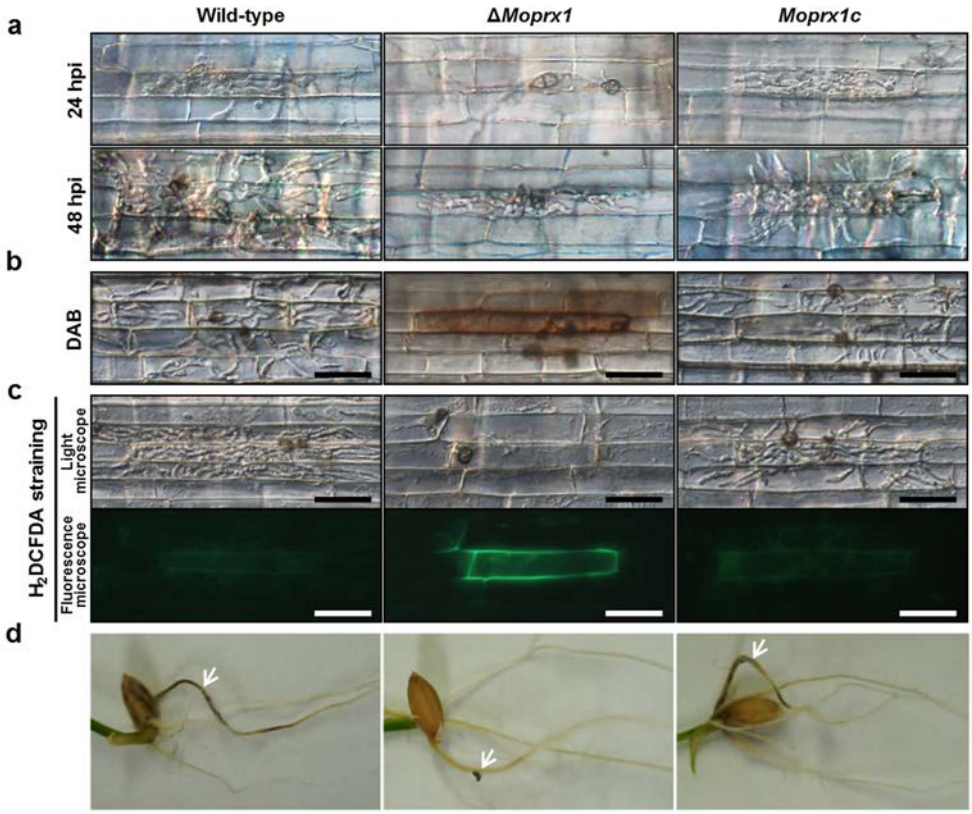

Figure 7. MoPRX1 detoxifies host ROS and is involved in rice root infection. (a) Sheath assays with compatible *Oryza sativa* L. cv. Nakdongbyeo showed delayed and restricted growth of Δ*MoPrx1* in rice cells. Sheaths were observed at 24 and 48 hpi inoculated with 2×10^4 conidia/ml. (b) ROS detection by DAB (3,3´-diaminobenzidine) staining, and (c) H_2DCFDA (5-(and-6)-chloromethyl-2′,7′-dichlorodihydrofluorescein diacetate acetyl ester) staining in inoculated rice sheaths at 48 hpi. DIC images were captured using a 20-ms exposure to transmitted light with a DIC filter. Fluorescence images were captured using a 200-ms exposure to absorbed light using a GFP filter.

Figure 7. (Continued)

Bar=50 μm. (d) Root infection from rice seedlings (*Oryza sativa* L. cv. Nakdongbyeo) by wild-type, Δ*Moprx1* and *MoPRX1c* strains. White arrow indicates the infection site on the root surface.

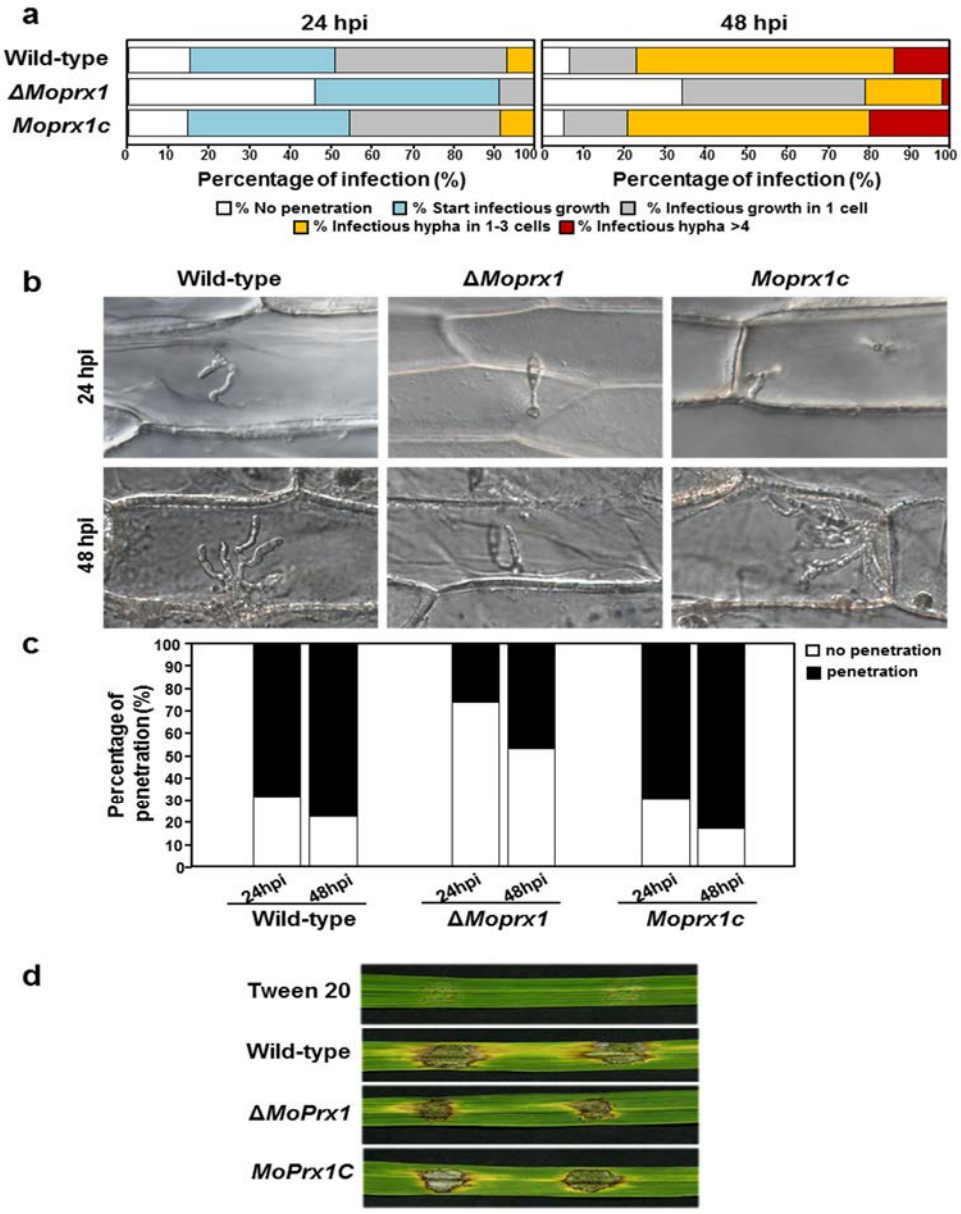

Figure 8. Penetration percentage and pathogenicity of *ΔMoprx1* on rice sheaths and leaves, and onion epidermal cells.

Figure 8. (Continued)

(a) Quantitative measurement of rice sheath assay by Δ*Moprx1*. Frequency was measured by counting three replicates of 75-100 appressoria. (b) Appressorial penetration assay on onion epidermal cell by drop inoculation with 2×10^4 conidia/ml and observed at 24 and 48 hpi. Images were captured using a 20-ms exposure to transmitted light with a DIC filter. (c) Percentage of appressorial penetration of onion epidermal cells. Data were obtained by counting three replicates of >100 appressoria. (d) Infiltration experiment on rice leaves. The conidial suspension used as an inoculum contained 5×10^4 conidia/ml. Photograph was taken at 5 dpi.

VII. Extracellular enzyme activity and transcription of other peroxidase genes can be perturbed by deletion of *MoPRX1*

From previous reports it is well known that extracellular peroxides activity play critical role in host derived ROS detoxification (Chi *et al.*, 2009a; Guo *et al.*, 2011a; Huang *et al.*, 2011)**.** As *ΔMoprx1* totally lost extracellular peroxidase activity in ABTS oxidizing test with CF (Figure 5c) next we target to assess enzyme activity in plate assay. Congo Red (CR) plate assay is used for cell wall protein assessment on plates and resulting red color degradation indicates extracellular peroxidase activity (Dalboge, 1997). Our results showed almost no red degradation halo in *ΔMoprx1* compared with the wild-type (Figure 9A), suggesting *ΔMoprx1* was defective in CR-degrading ability and lost extracellular peroxidase activity. Decreased laccase activity was observed in *ΔMoprx1*; for example, lower oxidized less purple color was observed relative to dark purple wild-type and complement strain (Figure 9B). It is well known Cu stimulate extracellular laccase activity. However, when 0.5 mM $CuSO_4$ was added to the medium, *ΔMoprx1* slightly restored laccase activity (Figure 9C).

The observation that ROS accumulation substantially increases in the absence of *MoPRX1* led us to examine the expression of a further 26 peroxidase genes using qRT-PCR in the Δ*Moprx1* background,

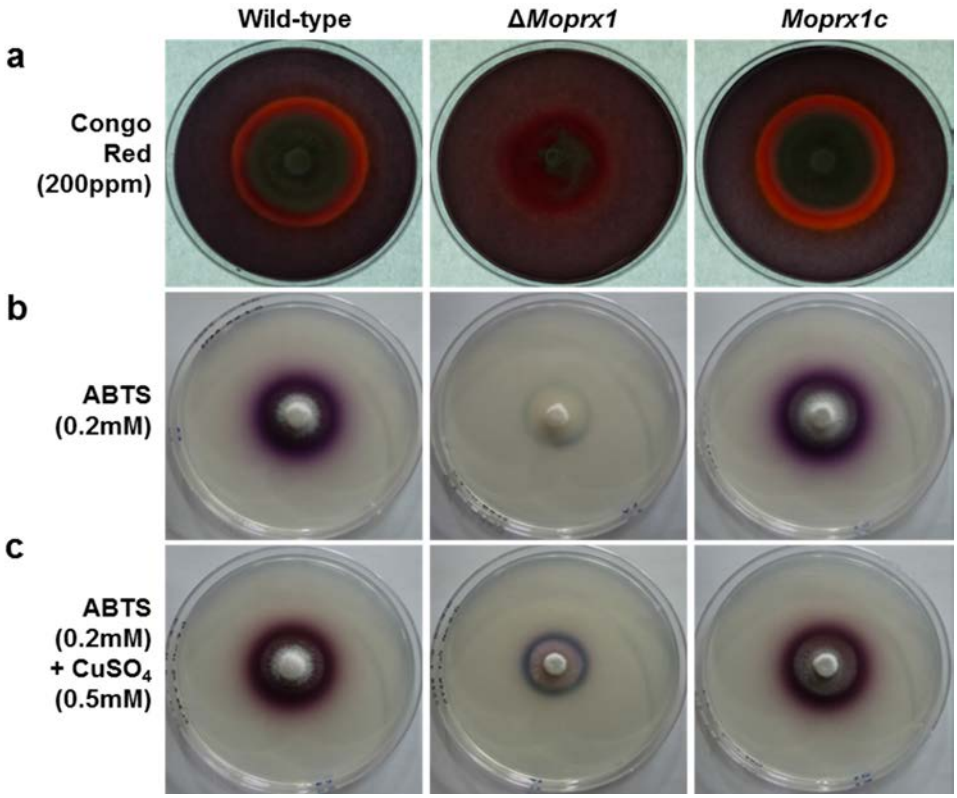

Figure 9. Extracellular enzyme activity in Δ*Moprx1*.

The wild-type, Δ*Moprx1*, and Moprx1c strains were inoculated on complete media (CM) containing (a) 200 ppm Congo Red, and (b) 0.2 mM ABTS, and (c) 0.2 mM ABTS with 0.5 mM $CuSO_4$. The 5-mm-diameter mycelial blocks were inoculated onto media, and incubated at 25°C. ABTS discoloration was observed at 4 dpi and Congo Red discoloration at 9 dpi.

compared to the wild-type. We included in this experiment *MoPRX1* to confirm absence of its transcripts in the mutant strain. Expression of *MoAPX1*, *MoLIP3*, *NOX1*, *NOX2*, *MoHPX2*, *MoHPX3*, *MoLDS1*, *MoPRX2*, *and MoVPX1* was upregulated (> 1.5-fold), whereas expression of *MoLIP1*, *MoLIP2*, *CATA*, *CATB* and *MoPRX3* was downregulated (< 0.5-fold) as shown in Figure 10. Expression of the remaining genes remained unchanged. No *MoPRX1* transcript was detected, as expected. CII peroxidases (*MoLIP1*, *MoLIP2*) and catalase (*CATB*), which are predicted to be secreted peroxidases having signal peptides (Table 4), were downregulated in Δ*Moprx1* (Figure 10). Our results showed that deletion of *MoPRX1* can alter transcript levels of other peroxidase genes and thus extracellular peroxidase activity.

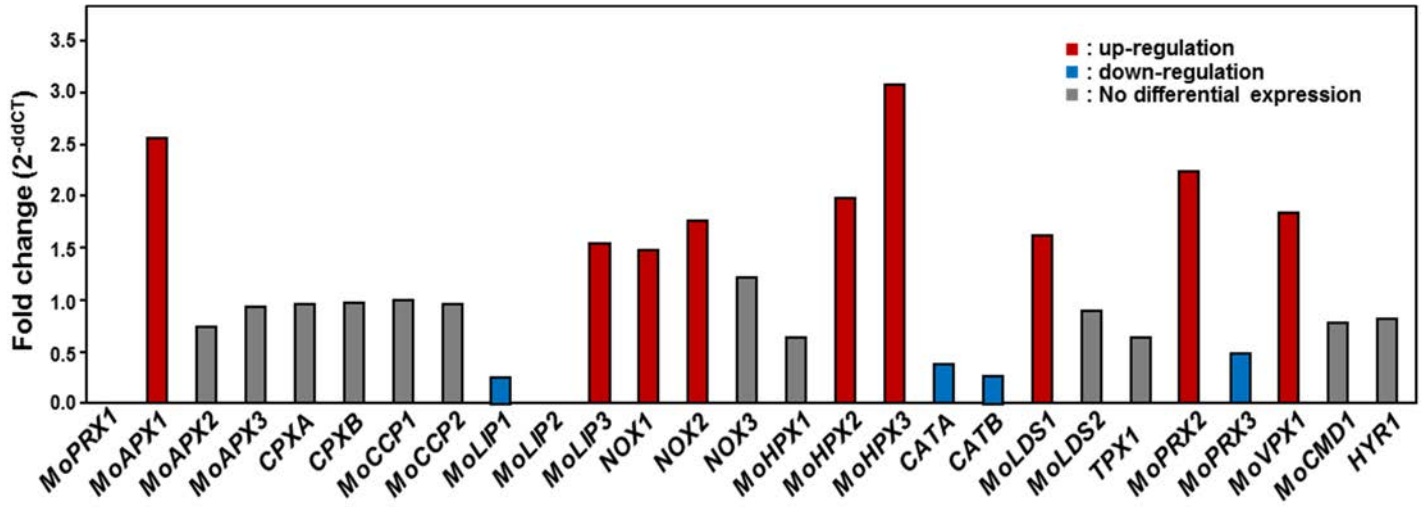

Figure 10. Expression profiles of 27 *M. oryzae* peroxidase genes in Δ*Moprx1*.

Upregulated genes (more than 1.5-fold) are indicated by red bars, and downregulated genes (less than 0.5-fold) are denoted by blue bars. The genes not showing differential expression are marked in gray.

DISCUSSION

Successful infection of hosts requires pathogens to be equipped with means to breach their defense strategies (Agrios, 1992; Chai *et al.*, 2009; Chi *et al.*, 2009a). The most prominent response of host plants to pathogen attack is a burst of ROS production. In response, pathogens have evolved antioxidant defense systems (Aguirre *et al.*, 2006). Recently, several studies have suggested that at least some of the peroxidases are integral components of such an antioxidant defense system in *M. oryzae* (Egan *et al.*, 2007; Skamnioti *et al.*, 2007; Huang *et al.*, 2011; Tanabe *et al.*, 2011; Fernandez and Wilson, 2014). Searching of the Fungal Peroxidase Database (fPoxDB) (Choi *et al.*, 2014) revealed 27 putative peroxidase genes encoded in the genome of *M. oryzae*, leaving the general role of peroxidases in fungal pathogenesis open to question. We classified those 27 putative peroxidase genes based on our phylogenetic analysis, and conducted functional analysis of a subset of the 27 genes.

Our expression profiling of 27 peroxidase genes showed that the majority (23 genes or 85%) of peroxidase genes were induced in infected plant samples (78 hpi), and 14 genes were upregulated under H_2O_2 stress (Figure 3). Seven peroxidase genes were upregulated during conidiation and 11 were upregulated

during appressoria formation. Considering that the host environment involved high levels of ROS, these data suggest that transcription of many peroxidases in *M. oryzae* is responsive to ROS, including H_2O_2.

For the biotrophic pathogens, *Claviceps purpurea* and *Ustilago maydis*, the transcription factor genes *CPTF1* and *YAP1*, respectively, were demonstrated to be required to cope with oxidative stresses (Nathues *et al.*, 2004; Molina and Kahmann, 2007). In *M. oryzae*, an ortholog of *YAP1*, *MoAP1*, was also shown to mediate oxidative stress responses (Guo *et al.*, 2011). Loss of these genes universally resulted in attenuated virulence. It is tempting to speculate that these transcription factors, in combination with others, would form a regulatory network shared by peroxidase genes in *M. oryzae*, explaining the common *in planta* transcriptional response among peroxidase genes. In support of this notion, microarray experiments on a *YAP1* deletion mutant showed that at least two peroxidase genes were regulated by *YAP1* in *U. maydis*.

We conducted functional analysis using targeted gene deletion for a set genes selected among the 27 genes. We basically selected genes from clades that did not contain previously characterized genes. Such an approach, in combination with knowledge of previously characterized genes, allowed us to evaluate the roles of peroxidase genes in fungal pathogenesis. Interestingly, all deletion

mutants of the seven genes displayed attenuated virulence compared to the wild-type.

We also observed that loss of the selected *M. oryzae* peroxidase genes resulted in decreased peroxidase activity and reduced tolerance to exogenous H_2O_2. Our correlation analysis of these attributes (pathogenicity, peroxidase activity, and sensitivity to exogenous H_2O_2) suggested that sensitivity to exogenous H_2O_2 could be a good proxy for pathogenicity defects ($r = 0.76$). It is noteworthy that deletion of 13 peroxidase genes to date (6 from previous studies and 7 from this study) led to attenuated virulence, without an exception. Such unanimous results suggest that all peroxidases are required for fungal pathogenesis, although their contributions vary widely.

Among the previously characterized genes, *NOX1* and *NOX2* were involved in regulation at the intracellular ROS level. For the remaining four genes, deletion of individual genes rendered the mutants sensitive to exogenous H_2O_2. This sensitivity to H_2O_2 correlated with the degree of fungal virulence, with the exception of *CPXB*, deletion of which had no effect on virulence. The reason that these mutants were impaired in virulence was not the loss of ability to detoxify or suppress host-driven ROS, except for *HYR1*. Nevertheless, fortifying the cell wall, as shown in the study of *CATB*, can be, though indirect, a means of coping with the fatal ROS-rampant environment. In most of the

mutants in our work developmental changes, including conidiation, conidial germination, and appressorium formation, were not significantly impaired. It is likely that all of the mutants were defective in the penetration or post-penetration phase. We confirmed that, at least in Δ*Moprx1*, the penetration process was not compromised. Considering the reduction in peroxidase activity and H_2O_2 tolerance, this suggests that the mutants were less pathogenic due to defects in coping directly or indirectly with host-driven ROS.

During our study, one of the mutants, Δ*Moprx1*, drew our attention because it was almost non-pathogenic to rice plants. *MoPRX1* was, based on sequence similarity, predicted as a gene encoding peroxiredoxin. In mammals, peroxiredoxins are known to be versatile. They possess antioxidant and chaperone-like activities, and, therefore, protect cells from oxidative insults (Rhee *et al.*, 2005). Moreover, they might directly interact with transcriptional factors such as c-Myc and NF-κB in the nucleus, and be secreted by some cells (Riddell *et al.*, 2010; Ishii *et al.*, 2012). Such versatility of mammalian counterparts and the dramatic defect in *ΔMoprx1* pathogenicity encouraged us to examine this mutant in more detail.

MoPRX1 was homologous to PRX1 (YBL064C) in *S. cerevisiae* (Table 3 and Table 4). PRX1 exerts protective antioxidant roles in a cell through its peroxidase activity in detoxifying ROS (Bryk *et al.*, 2000; Peshenko and Shichi,

2001; Hofmann *et al.*, 2002). In *S. cerevisiae*, *PRX1* expression is induced in response to oxidative stress and activation of respiratory pathways (Pedrajas *et al.*, 2000). Similarly, the *PRX1* gene in the human pathogenic fungi, *A. fumigatus* and *C. albicans*, was also induced after H_2O_2 exposure(Lessing *et al.*, 2007; Srinivasa *et al.*, 2012). Unlike *S. cerevisiae* and human pathogenic fungi, however, we found that *MoPRX1* expression was not induced in the presence of exogenous H_2O_2, but during appressorial development and infection at 78 hpi (Figure 3). Furthermore, MoPRX1 seemed to be present in cytoplasm regardless of developmental changes. *In silico* analysis of *S. cerevisae* PRX1 and MoPRX1 using PSortII(Nakai and Horton, 1999), TargetP (Emanuelsson *et al.*, 2000), and Mitoprot (Claros and Vincens, 1996) predicted unanimously that PRX1 would be localized to mitochondria while MoPRX1 to cytoplasm and mitochondrial-targeting signal (MTS) (Rapaport, 2003) was not found in MoPRX1 , suggesting that cytoplasmic localization of MoPRX1 is less likely to be artifact.

This was in contrast to *S. cerevisiae* PRX1, which was shown to localize to mitochondria and *C. albicans* PRX1 that translocated from cytoplasm to the nucleus during hyphal transition. Despite such differences, *MoPRX1* could complement hypersensitivity of the *PRX1* deletion mutant of *S. cerevisiae*, indicating functional conservation as a peroxiredoxin. Although expression of *MoPRX1* was not induced in response to exogenous H_2O_2, the deletion mutant

was extremely sensitive to this exogenous H_2O_2, suggesting that *MoPRX1* might be constitutively expressed to function at the front line against oxidative stresses. Another interesting speculation regarding MoPRX1 is that it mainly functions as a general protective barrier against ROS in cytoplasm, while its orthologs detoxify ROS in tight association with metabolic or developmental cell changes. Our data suggest that the functions of PRX1 as a peroxiredoxin have been co-opted depending on the lifestyle of the fungal species.

Using DAB and H_2DCFDA staining's of rice sheaths during infection; we showed that *MoPRX1* is required to incapacitate host-derived ROS *in planta*. Our localization analysis of MoPRX1 raised the question of how MoPRX1 removes host-derived ROS while they are present in the fungal cytoplasm. This is reminiscent of recent reports from studies focusing on *DES1* and *HYR1* (Chi *et al.*, 2009a; Huang *et al.*, 2011). DES1 and HYR1 were not secreted into the extracellular milieu, yet they could detoxify/suppress ROS generated by the host plant as a defense response. One possible explanation is that *MoPRX1* regulated other ROS-related genes, such as peroxidases and laccases, as suggested in the case of *DES1* and *HYR1*. In support of this, we found that deletion of *MoPRX1* resulted in loss of extracellular peroxidase and laccase activity (Figure 9), as well as causes perturbations in the transcription of other peroxidase genes (Figure 10).

In humans, a peroxiredoxin was shown to function as a molecular chaperone (Welch and Brown, 1996; Jang *et al.*, 2004; Lee *et al.*, 2007). Alternatively, it is, therefore, possible that MoPRX1 also acts as a molecular chaperone that is involved in processing secreted proteins. The second possibility is not mutually exclusive to the first and should be an interesting topic for future studies.

In conclusion, we systematically identified and characterized peroxidase genes in the rice blast fungus. Combining a phylogenetic approach with expression profiling and gene deletion, our work provided not only a comprehensive view of the contributions made by peroxidase genes to fungal pathogenesis but also insights into infection strategy built on evolutionarily conserved peroxidases in the fungus. Furthermore, our study posed important questions regarding how the peroxidase-mediated system is regulated at the transcriptional level and the relationships among peroxidases and novel factors, such as *DES1*. These issues should be addressed in future studies to elucidate ROS-scavenging pathways in fungi pathogenic to plants.

LITERATURE CITED

Agrios, G. N. 1992. Frontiers and challenges in plant pathology communications. *Phytopathol*. 82: 32-34.

Aguirre, J., Hansberg, W. and Navarro, R. 2006. Fungal responses to reactive oxygen species. *Med*. *Mycol*. 44: S101-S107.

Auh, C.-K. and Murphy, T. M. 1995. Plasma membrane redox enzyme is involved in the synthesis of O^{2-} and H_2O_2 by *Phytophthora* elicitor-stimulated rose cells. *Plant*. *Physiol*. 107: 1241-1247.

Bolwell, G. P. and Wojtaszek, P. 1997. Mechanisms for the generation of reactive oxygen species in plant defence-a broad perspective. *Physiol*. *Mol*. *Plant Pathol*. 51: 347-366.

Bradley, D. J., Kjellbom, P. and Lamb, C. J. 1992. Elicitor- and wound-induced oxidative cross-linking of a proline-rich plant cell wall protein: a novel, rapid defense response. *Cell* 70:21-30.

Bryk, R., Griffin, P. and Nathan, C. 2000. Peroxynitrite reductase activity of baterial peroxiredoxns. *Nature* 407: 211-215.

Chai, L. Y. A., Netea, M. G., Vonk, A. G. and Kullberg, B. J. 2009. Fungal strategies for overcoming host innate immune response. *Med*. *Mycol*. 47: 227-236.

Chi, M. H., Park, S. Y., Kim, S. and Lee, Y. H. 2009a. A novel pathogenicity gene is required in the rice blast fungus to suppress the basal defenses of the host. *PLoS Pathog*. 5(4):e1000401.

Chi, M. H., Park, S. Y. and Lee, Y. H. 2009b. A quick and safe method for fungal DNA extraction. *Plant Pathol. J*. 25:108-111.

Choi, J., Detry, N., Kim, K. T., Asiegbu, F. O., Valkonen, J. P. T. and Lee, Y. H. 2014. fPoxDB: fungal peroxidase database for comparative genomics. *BMC Microbiol*. 14:117.

Claros, M. G. and Vincens, P. 1996. Computational method to predict mitochondrially imported proteins and their targeting sequences. *Eu. J. Biochem*. 241: 779-786.

Dalboge, H. 1997. Expression cloning of fungal enzyme genes; a novel approach for efficient isolation of enzyme genes of industrial relevance. *FEMS Microbiol. Rev*. 21:29-42.

Davidson, J. F., Whyte, B., Bissinger, P. H. and Schiestl, R. H. 1996. Oxidative stress is involved in heat-induced cell death in *Saccharomyces cerevisiae*. *Proc. Natl. Acad. Sci. U. S. A*. 93:5116-5121.

Dean, R. A., Talbot, N. J., Ebbole, D. J., Farman, M. L., Mitchell, T. K., Orbach, M. J., Thon, M., Kulkarni, R., Xu, J. R., Pan, H., Read, N. D., Lee, Y. H., Carbone, I., Brown, D., Oh, Y. Y., Donofrio, N., Jeong, J. S., Soanes,

D. M., Djonovic, S., Kolomiets, E., Rehmeyer, C., Li, W., Harding, M., Kim, S., Lebrun, M. H., Bohnert, H., Coughlan, S., Butler, J., Calvo, S., Ma, L. J., Nicol, R., Purcell, S., Nusbaum, C., Galagan, J. E. and Birren, B. W. 2005. The genome sequence of the rice blast fungus *Magnaporthe grisea*. *Nature* 434:980-6.

Dietz, K. J., Jacob, S., Oelze, M. L., Laxa, M., Tognetti, V., de Miranda, S. M., Baier, M. and Finkemeier, I. 2006. The function of peroxiredoxins in plant organelle redox metabolism. *J. Exp. Bot.* 57:1697-709.

Doke, N. 1983. Involvement of superoxide anion generation in the hypersensitive response of potato tuber tissues to infection with an incompatible race of *Phytophthora infestans* and to the hyphal wall components. *Physiol*. *Plant Pathol*. 23: 345-357.

Edgar, R. S., Green, E.W., Zhao, Y., van Ooijen, G., Olmedo, M., Qin, X., Xu, Y., Pan, M., Valekunja, U. K., Feeney, K. A., Maywood, E. S., Hastings, H. S.. Baliga, N. S., Merrow, M., Millar, A. J., Johnson, C. H., Kyriacou, C. P., O'Neill, J. S. and Reddy, A. B. 2012. Peroxiredoxins are conserved markers of circadian rhythms. *Nature* 485: 459-464.

Egan, M. J., Wang, Z. Y., Jones, M. A., Smirnoff, N. and Talbot, N. J. 2007. Generation of reactive oxygen species by fungal NADPH oxidases is required for rice blast disease. *Proc. Natl. Acad. Sci. U. S. A.* 104:11772-

7.

Emanuelsson, O., Nielsen, H., Brunak, S. and von Heijne, G. 2000. Predicting subcellular localization of proteins based on their N-terminal amino acid sequence. *J. Mol. Biol.* 300: 1005-1016.

Enjalbert, B., MacCallum, D. M., Odds, F. C. and Brown, A. J. P. 2007. Niche-specific activation of the oxidative stress response by the pathogenic fungus *Candida albicans*. *Infect. Immun.* 75:2143-2151.

Fernandez, J. and Wilson, R. A. 2014. Characterizing roles for the glutathione reductase, thioredoxin reductase and thioredoxin peroxidase-encoding genes of *Magnaporthe oryzae* during rice blast disease. *PLoS ONE* 9(1):e87300.

Fisher, M. C., Henk, D. A., Briggs, C. J., Brownstein, J. S., Madoff, L. C., McCraw, S. L. and Gurr, S. J. 2012. Emerging fungal threats to animal, plant and ecosystem health. *Nature* 484: 186-194.

Fourquet, S., Huang, M. E., D'Autreaux, B. and Toledano, M. B. 2008. The dual functions of thiol-based peroxidases in H_2O_2 scavenging and signaling. *Antioxid. Redox Signal* 10:1565-76.

Grant, M., Brown, I., Adams, S., Knight, M., Ainslie, A. and Mansfield, J. 2000. The RPM1 plant disease resistance gene facilitates a rapid and sustained increase in cytosolic calcium that is necessary for the oxidative burst and

hypersensitive cell death. *Plant J*. 23: 441-450.

Guo, M., Chen, Y., Du, Y., Dong, Y., Guo, W., Zhai, S., Zhang, H., Dong, S., Zhang, Z., Wang, Y., Wang, P. and Zheng, X. 2011. The bZIP transcription factor *MoAP1* mediates the oxidative stress response and is critical for pathogenicity of the rice blast fungus *Magnaporthe oryzae*. *PLoS Pathog*. 7(2):e1001302.

Heller, J., Meyer, A. J. and Tudzynski, P. 2012. Redox-sensitive GFP2: use of the genetically encoded biosensor of the redox status in the filamentous fungus *Botrytis cinerea*. *Mol*. *Plant Pathol*. 13: 935-947.

Heller, J. and Tudzynski, P. 2011. Reactive oxygen species in phytopathogenic fungi: signaling, development, and disease. *Annu*. *Rev*. *Phytopathol*. 49: 369-390.

Hofmann, B., Hecht H. J. and Flohe, L. 2002. Peroxiredoxins. *Biol*. *Chem*. 383: 347-364

Howard, R. J., Ferrari, M. A., Roach, D. H. and Money, N. P. 1991. Penetration of hard substrates by a fungus employing enormous turgor pressures. *Proc*. *Natl. Acad. Sci. U. S. A*. 88: 11281-11284.

Huang, K., Czymmek, K. J., Caplan, J. L., Sweigard, J. A. and Donofrio, N. M. 2011. *HYR1*-mediated detoxification of reactive oxygen species is required for full virulence in the rice blast fungus. *PLoS Pathog*.

7(4):e1001335.

Huckelhoven, R. 2007. Cell wall - associated mechanisms of disease resistance and susceptibility. *Annu. Rev. Phytopathol*. 45:101-127.

Ishii, T., Warabi, E. and Yanagawa, T. 2012. Novel roles of peroxiredoxins in inflammation, cancer and innate immunity. *J. Clin. Biochem. Nutri*. 50: 91-105.

Jang, H. H., Lee, K. O., Chi, Y. H., Jung, B. G., Park, S. K., Park, J. H., Lee, J. R., Lee, S. S., Moon, J. C., Yun, J. W., Choi, Y. O., Kim, W. Y., Kang, J. S., Cheong, G. W., Yun, D. J., Rhee, S. G., Cho, M. J. and Lee, S. Y. 2004. Two enzymes in one; two yeast peroxiredoxins display oxidative stress-dependent switching from a peroxidase to a molecular chaperone function. *Cell* 117:625-35.

Jones, J. D. and Dangl, J. L. 2006. The plant immune system. *Nature* 444:323-9.

Kankanala, P., Czymmek, K. and Valent, B. 2007. Roles for rice membrane dynamics and plasmodesmata during biotrophic invasion by the blast fungus. *Plant Cell* 19:706-24.

Kim, K. H., Willger, S. D., Park, S. W., Puttikamonkul, S., Grahl, N., Cho, Y., Mukhopadhyay, B., Cramer, R. A., Jr. and Lawrence, C. B. 2009. TmpL, a transmembrane protein required for intracellular redox homeostasis

and virulence in a plant and an animal fungal pathogen. *PLoS Pathog*. 5(11):e1000653.

Kim, S., Park, S. Y., Kim, K. S., Rho, H. S., Chi, M. H., Choi, J., Park, J., Kong, S., Park, J., Goh, J. and Lee, Y. H. 2009. Homeobox transcription factors are required for conidiation and appressorium development in the rice blast fungus *Magnaporthe oryzae*. *PLoS Genet*. 5(12):e1000757.

Koga, H., Dohi, K., Nakayachi, O. and Mori, M. 2004. A novel inoculation method of *Magnaporthe grisea* for cytological observation of the infection process using intact leaf sheaths of rice plants. *Physiol. Mol. Plant Pathol*. 64:67-72.

Lamb, C. and Dixon, R. A. 1997. The Oxidative Burst in Plant Disease Resistance. *Annu. Rev. Plant. Physiol. Plant. Mol. Biol*. 48: 251-275.

Koua, D., Cerutti, L., Falquet, L., Sigrist, C. J., Theiler, G., Hulo, N. and Dunand, C. 2009. PeroxiBase: a database with new tools for peroxidase family classification. *Nucleic Acids Res*. 37:D261-6.

Lee, W. S., Choi, K. S., Riddell, J., Ip, C., Ghosh, D., Park, J. H. and Park, Y. M. 2007. Human peroxiredoxin 1 and 2 are not duplicate proteins - The unique presence of Cys(83) in Prx1 underscores the structural and functional differences between Prx1 and Prx2. *J. Biol. Chem*. 282: 22011-22022.

Lessing, F., Kniemeyer, O., Wozniok, W., Loeffler, J., Kurzai, O., Haertl, A. and Brakhage, A. A. 2007. The *Aspergillus fumigatus* transcriptional regulator *AfYap1* represents the major regulator for defense against reactive oxygen intermediates but is dispensable for pathogenicity in an intranasal mouse infection model. *Eukaryot*. *Cell* 6:2290-2302.

Levine, A., Tenhaken, R., Dixon, R. and Lamb, C. 1994. H_2O_2 from the oxidative burst orchestrates the plant hypersensitive disease resistance response. *Cell* 79:583-93.

Lin, C. H., Yang, S. L. and Chung, K. R. 2009. The YAP1 homolog-mediated oxidative stress tolerance is crucial for pathogenicity of the necrotrophic fungus *Alternaria alternata* in citrus. *Mol*. *Plant-Microbe Interact*. 22:942-952.

Livak, K. J. and Schmittgen, T. D. 2001. Analysis of relative gene expression data using real-time quantitative PCR and the 2(T)(-Delta Delta C) method. *Methods* 25:402-408.

Missall, T. A., Pusateri, M. E. and Lodge, J. K. 2004. Thiol peroxidase is critical for virulence and resistance to nitric oxide and peroxide in the fungal pathogen, *Cryptococcus neoformans*. *Mol Microbiol*. 51:1447-58.

Molina, L. and Kahmann, R. 2007. An *Ustilago maydis* gene involved in H_2O_2 detoxification is required for virulence. *Plant Cell* 19:2293-309.

Nakai, K. and Horton, P. 1999. PSORT: a program for detecting sorting signals in proteins and predicting their subcellular localization. *Trends Biochem. Sci*. 24: 34-35.

Nathues, E., Joshi, S., Tenberge, K. B., von den Driesch, M., Oeser, B., Baumer, N., Mihlan, M. and Tudzynski, P. 2004. CPTF1, a CREB-like transcription factor, is involved in the oxidative stress response in the phytopathogen *Claviceps purpurea* and modulates ROS level in its host *Secale cereale*. *Mol. Plant-Microbe Interact*. 17: 383-393.

Park, S. Y., Choi, J., Lim, S. E., Lee, G. W., Park, J., Kim, Y., Kong, S., Kim, S. R., Rho, H. S., Jeon, J., Chi, M. H., Kim, S., Khang, C. H., Kang, S. and Lee, Y. H. 2013. Global expression profiling of transcription factor genes provides new insights into pathogenicity and stress responses in the rice blast fungus. *PLoS Pathog*. 9(6):e1003350.

Park, S. Y., Milgroom, M. G., Han, S. S., Kang, S. and Lee, Y. H. 2003. Diversity of pathotypes and DNA fingerprint haplotypes in populations of *Magnaporthe grisea* in Korea over two decades. *Phytopathol*.93:1378-1385.

Passardi, F., Theiler, G., Zamocky, M., Cosio, C., Rouhier, N., Teixera, F., Margis-Pinheiro, M., Ioannidis, V., Penel, C., Falquet, L. and Dunand, C. 2007. PeroxiBase: the peroxidase database. *Phytochem*. 68:1605-11.

Pedrajas, J. R., Miranda-Vizuete, A., Javanmardy, N., Gustafsson, J. A. and Spyrou, G. 2000. Mitochondria of *Saccharomyces cerevisiae* contain one-conserved cysteine type peroxiredoxin with thioredoxin peroxidase activity. *J. Biol. Chem*. 275:16296-301.

Peshenko, I. V. and Shichi, H. 2001. Oxidation of active center cysteine of bovine 1-Cys peroxiredoxin to the cysteine sulfenic acid form by peroxide and peroxynitrite. *Free Radical Bio. Med*. 31: 292-303.

Rapaport, D. 2003. Finding the right organelle - targeting signals in mitochondrial outer-membrane proteins. *EMBO Rep*. 4: 948-952.

Rhee, S. G., Chae, H. Z. and Kim, K. 2005. Peroxiredoxins: a historical overview and speculative preview of novel mechanisms and emerging concepts in cell signaling. *Free Radical Bio. Med.* 38:1543-52.

Rhee, S. G., Woo, H. A., Kil, I. S. and Bae, S. H. 2012. Peroxiredoxin functions as a peroxidase and a regulator and sensor of local peroxides. *J Biol. Chem*. 287(7): 4403-4410.

Riddell, J. R., Wang, X. Y., Minderman, H. and Gollnick, S. O. 2010. Peroxiredoxin 1 stimulates secretion of proinflammatory cytokines by binding to TLR4. *J. Immunol.* 184:1022-1030.

Samalova, M., Meyer, A. J., Gurr, S. J. and Fricker, M. D. 2014. Robust anti-oxidant defences in the rice blast fungus *Magnaporthe oryzae* confer

tolerance to the host oxidative burst. *New Phytologist* 201: 556-573.

Sesma, A. and Osbourn, A. E. 2004. The rice leaf blast pathogen undergoes developmental processes typical of root- infecting fungi. *Nature* 431: 582-586.

Schiestl, R. H. and Gietz, R. D. 1989. High-efficiency transformation of intact yeast-cells using single stranded nucleic-acids as a carrier. *Curr*. *Genet*. 16:339-346.

Skamnioti, P., Henderson, C., Zhang, Z., Robinson, Z. and Gurr, S. J. 2007. A novel role for catalase B in the maintenance of fungal cell-wall integrity during host invasion in the rice blast fungus *Magnaporthe grisea*. *Mol .Plant Microbe Interact*. 20:568-80.

Srinivasa, K., Kim, N. R., Kim, J., Kim, M., Bae, J. Y., Jeong, W., Kim, W. and Choi, W. 2012. Characterization of a putative thioredoxin peroxidase *Prx1* of *Candida albicans*. *Mol*. *Cells* 33:301-307.

Talbot, N. J. 2003. On the trail of a cereal killer: Exploring the biology of *Magnaporthe grisea*. *Annu*. *Rev*. *Microbiol*. 57:177-202.

Talbot, N. J., McCafferty, H. R. K., Ma, M., Moore, K. and Hamer, J. E. 1997. Nitrogen starvation of the rice blast fungus *Magnaporthe grisea* may act as an environmental cue for disease symptom expression. *Physiol*. *Mol*. *Plant Pathol*. 50:179-195.

Tamura, K., Stecher, G., Peterson, D., Filipski, A. and Kumar, S. 2013. MEGA6: molecular evolutionary genetics analysis version 6.0. *Mol. Biol. Evol.* 30:2725-2729.

Tanabe, S., Ishii-Minami, N., Saitoh, K., Otake, Y., Kaku, H., Shibuya, N., Nishizawa, Y. and Minami, E. 2011. The role of catalase-peroxidase secreted by *Magnaporthe oryzae* during early infection of rice cells. *Mol. Plant-Microbe Interact.* 24:163-71.

Torres, M. A., Jones, J. D. and Dangl, J. L. 2005. Pathogen-induced, NADPH oxidase-derived reactive oxygen intermediates suppress spread of cell death in *Arabidopsis thaliana*. *Nat. Genet.* 37:1130-4.

Tudzynski, P., Heller, J. and Siegmund, U. 2012. Reactive oxygen species generation in fungal development and pathogenesis. *Curr. Opin. Microbiol*. 15: 653-659.

Welch, W. J. and Brown, C. R. 1996. Influence of molecular and chemical, chaperones on protein folding. *Cell Stress Chaperone.*1(2): 109-115.

Wojtaszek, P. 1997. Oxidative burst: an early plant response to pathogen infection. *Biochem. J.* 322:681-92.

Yu, J. H., Hamari, Z., Han, K. H., Seo, J. A., Reyes-Dominguez, Y. and Scazzocchio, C. 2004. Double-joint PCR: a PCR-based molecular tool for gene manipulations in filamentous fungi. *Fungal Genet. Biol.*

41:973-981.

Yun, S. H. 1998. Molecular genetics and manipulation of pathogenicity and mating determinants in *Cochliobolus heterostrophus* and *Mycosphaerella zeae-maydis*. PhD Thesis, Cornell University.